JEM Journal of Experimental Medicine

ARTICLE

Peripheral PDGFRα⁺gp38⁺ mesenchymal cells support the differentiation of fetal liver–derived ILC2

Satoshi Koga[1,3], Katsuto Hozumi[4], Ken-ichi Hirano[4], Masaki Yazawa[4,5], Tommy Terooatea[6], Aki Minoda[6], Takashi Nagasawa[7], Shigeo Koyasu[2,8], and Kazuyo Moro[1,2,3]

Group 2 innate lymphoid cells (ILC2s) are derived from common lymphoid progenitors (CLPs) via several specific precursors, and the transcription factors essential for ILC2 differentiation have been extensively studied. However, the external factors regulating commitment to the ILC lineage as well as the sites and stromal cells that constitute the optimal microenvironment for ILC2-specific differentiation are not fully defined. In this study, we demonstrate that three key external factors, the concentration of interleukin 7 (IL-7) and strength and duration of Notch signaling, coordinately determine the fate of CLP toward the T, B, or ILC lineage. Additionally, we identified three stages of ILC2 in the fetal mesentery that require STAT5 signals for maturation: ILC progenitors, CCR9⁺ ILC2 progenitors, and KLRG1⁻ immature ILC2. We further demonstrate that ILC2 development is supported by mesenteric platelet-derived growth factor receptor α (PDGFRα)⁺ glycoprotein 38 (gp38)⁺ mesenchymal cells. Collectively, our results suggest that early differentiation of ILC2 occurs in the fetal liver via IL-7 and Notch signaling, whereas final differentiation occurs in the periphery with the aid of PDGFRα⁺gp38⁺ cells.

Introduction

Innate lymphoid cells (ILCs) are antigen-independent effector cells that are a counterpart of T cell subsets. ILCs are categorized into three groups based on their cytokine profile and transcription factors controlling their differentiation and function: group 1 ILC (ILC1), group 2 ILC (ILC2), and group 3 ILC (ILC3; Spits et al., 2013). ILC2s are type 2 cytokine producers that produce IL-4, IL-5, IL-6, IL-9, IL-13, and GM-CSF in response to mucosal tissue-derived cytokines, including IL-25, IL-33, and thymic stromal cell lymphopoietin (TSLP), and play crucial roles in helminth infection, allergic inflammation, and tissue homeostasis (Artis and Spits, 2015; Ealey et al., 2017).

To understand the mechanism of ILC2 differentiation, many studies have focused on ILC-specific progenitors and transcription factors. In addition to T cells and B cells, all ILCs including ILC2 are derived from common lymphoid progenitors (CLPs; Yang et al., 2011) in the fetal liver (FL) and bone marrow (BM). Recently, ILC-committed progenitors such as early innate lymphoid progenitors (EILPs; Yang et al., 2015), CXCR6⁺ α–lymphoid progenitors (Yu et al., 2014), common progenitor to all helper-like ILCs (CHILPs; Klose et al., 2014), and PLZF⁺ ILC progenitors (ILCPs; Constantinides et al., 2014) have been identified. Several key transcription factors such as Id2, Tox, TCF-1, and Nfil3 have been reported to play a role in the lineage commitment from CLP (De Obaldia and Bhandoola, 2015; Zook and Kee, 2016). However, the microenvironmental factors in the developmental niches that regulate these transcription factors and promote ILC-specific differentiation from common progenitors are still unclear. All lymphocytes, with the exception of IL-15–dependent natural killer (NK) cells, require IL-7 for differentiation (Ma et al., 2006; Moro et al., 2010; Hong et al., 2012; Hoyler et al., 2012; Clark et al., 2014), and Notch signaling is essential for T cell, ILC2, and ILC3 development (Hozumi et al., 2008; Possot et al., 2011; Wong et al., 2012). It remains unclear, however, how these identical external factors determine the cell fate of the ILC lineage from CLP.

Furthermore, little is known about the site of ILC2 development. A previous study showed that KLRG1⁻ ILC2s exist in BM and that these cells are considered ILC2 progenitors (ILC2P; Hoyler et al., 2012). Therefore, it is generally thought that ILC2s are derived from BM even though CLP and ILCPs also exist in the FL, and studies on ILC2 differentiation have mainly been

[1]Laboratory for Innate Immune Systems, RIKEN Center for Integrative Medical Sciences, Yokohama, Japan; [2]Laboratory for Immune Cell Systems, RIKEN Center for Integrative Medical Sciences, Yokohama, Japan; [3]Division of Immunobiology, Department of Medical Life Science, Department of Supramolecular Biology, Graduate School of Medical Life Science, Yokohama City University, Yokohama, Japan; [4]Department of Immunology, Tokai University School of Medicine, Isehara, Japan; [5]Department of Biochemistry, Tokai University, Hiratsuka, Japan; [6]Epigenome Technology Exploration Unit, RIKEN Center for Life Science Technologies, Yokohama, Japan; [7]Laboratory of Stem Cell Biology and Developmental Immunology, Graduate School of Frontier Biosciences and Graduate School of Medicine, World Premier International Immunology Frontier Research Center, Osaka University, Suita, Japan; [8]Deparment of Microbiology and Immunology, Keio University School of Medicine, Tokyo, Japan.

Correspondence to Kazuyo Moro: kazuyo.moro@riken.jp.

conducted using BM progenitors. However, mature ILC2s exist in a variety of tissues such as adipose tissue, lung, gut, and skin. Parabiosis studies have clearly shown that ILC2 are tissue-resident cells, and ILC2 and ILCP do not circulate between tissues in the steady-state condition (Gasteiger et al., 2015; Moro et al., 2016). These data suggest that BM progenitors might not be the source of ILC2 in the steady-state and indicate the possibility that ILC2s differentiate from CLP in the FL.

It has been demonstrated that FoxN1$^+$ thymic epithelial cells constitute an essential microenvironment for T cell development (Žuklys et al., 2016), and BM CXCL12-abundant reticular cells support B cell differentiation in the BM niche (Tokoyoda et al., 2004; Nagasawa, 2007). However, determining what types of mesenchymal cells support the final differentiation of ILC2s in peripheral tissues has remained largely unexplored. If ILC2s differentiate from CLP in the FL and migrate into the peripheral tissues, specific stromal cells that provide an optimal microenvironment for ILC2 differentiation should exist in each tissue.

In this study, we determined whether the quantity of IL-7 and Notch signaling differentially regulated commitment to each lymphocyte lineage from CLP in the FL using a TSt4 stromal cell–based in vitro culture system and demonstrated that the concentration of IL-7 and strength and duration of Notch signaling differentially optimized the commitment to each lymphocyte lineage. In an in vivo analysis, thymic epithelial cell–specific Notch ligand deficiency in mice clearly led to abnormal expansion of ILC2 in the thymus, suggesting the importance of Notch signaling for lymphocyte lineage commitment in vivo. We hypothesized that after the first cell fate decision step occurred in the FL, CHILP/ILCP migrated into the peripheral tissues such as the mesentery, lung, or intestine and differentiated into mature ILC2 with the help of mesenchymal cells. In this study, we found that ILCs, immature ILCs including CCR9$^+$ ILC2 progenitors, and KLRG1$^-$ immature ILC2s exist in the fetal mesentery and that their maturation occurs after birth with the aid of STAT5 activators. We also identified CD45$^-$CD31$^-$ platelet-derived growth factor receptor α (PDGFRα)$^+$ glycoprotein 38 (gp38)$^+$ mesenchymal cells in the fetal and adult mesentery, which support ILC2 differentiation and maturation. Notably, CD45$^-$CD31$^-$PDGFRα$^+$gp38$^+$ mesenchymal cells support ILC2 differentiation from the ILCP but not CLP stage. These results demonstrate that the peripheral microenvironment plays a crucial role in the terminal differentiation of tissue-resident ILC2.

Results

Different concentrations of IL-7 optimize the cell fate of T cell, B cell, and ILC lineages

IL-7 is a critical cytokine for most lymphocytes, and previous research has shown that IL-7 concentration affects T cell differentiation (Ikawa et al., 2010). To determine whether IL-7 concentration also affects the differentiation of other lymphocytes, we cocultured E15 FL CLP with TSt4–Delta-like (DLL)–1 stromal cells, which express the Notch ligand DLL1, in the presence of different concentrations of IL-7. After 10 d of coculture, we found that low concentrations of IL-7 promoted CD4$^+$CD8α$^+$ double-positive (DP) T cell differentiation as previously reported (Fig. 1, A and B; Ikawa et al., 2010). However, high concentrations of IL-7 promoted the differentiation of GATA3^{hi} ILC2 (Fig. 1, A and B; and not depicted). A STAT5 inhibitor that blocks IL-7 signaling (Rochman et al., 2009) inhibited ILC2 differentiation, whereas T cell differentiation was only affected by high concentrations of the inhibitor (Fig. 1, C and D). These data indicate that both T cells and ILC2 require IL-7 but that the concentration of IL-7 differentially determines the commitment to T cells or ILC2. We also examined the differentiation of B cells, NK/ILC1, and ILC3 in different concentrations of IL-7. Lymphoid tissue inducer (LTi) cells are able to develop without Notch signaling (Possot et al., 2011), and ILC3s express low levels of GATA3 (Serafini et al., 2014). We therefore defined RORγt$^+$GATA3^{lo} cells as LTi-like cells and RORγt$^+$GATA3^{mid} cells as ILC3-like cells in the TSt4 and TSt4-DLL1 culture systems, respectively. Although LTi cell differentiation required high concentrations of IL-7, ILC3 differentiated efficiently at low concentrations of IL-7, as did T cells (Fig. 1, E and F). In this culture system, it is difficult to clearly distinguish between NK cells and ILC1. High concentrations of IL-7 promoted NK1.1$^+$ cell (NK/ILC1) differentiation in both the TSt4 and TSt4-DLL1 culture systems, whereas B cell differentiation was unaffected by the concentration of IL-7 in the TSt4 culture system (Fig. 1, G–I).

The strength of Notch signaling differentially regulates lymphocyte lineage commitment

Given that Notch signaling supports the commitment to T cell differentiation (Washburn et al., 1997; Han et al., 2002; De Smedt et al., 2005), we investigated the influence of Notch signal strength on lymphocyte commitment using newly established TSt4-based cell lines (TSt4 Tet-off DLL stromal cell system). Although both DLL1 and DLL4 can induce T cell differentiation, their efficiencies are quite different (Besseyrias et al., 2007; Mohtashami et al., 2010; Andrawes et al., 2013). Therefore, in this study, we used both TSt4 Tet-off DLL1 and DLL4 stromal cells. In these cell lines, DLL1 (Fig. 2) or DLL4 (Fig. 3) is expressed on TSt4 cells in the absence of doxycycline (Dox), and DLL expression can be down-regulated by Dox in a dose-dependent manner. CLPs were cocultured with these stromal cells with 10 ng/ml IL-7 and different concentrations of Dox (Figs. 2 A and 3 A). B cell differentiation from CLP was preferentially induced by coculture with both TSt4 Tet-off DLL1 and DLL4 stromal cells at high concentrations of Dox, which indicates weak Notch signaling (Fig. 2, B and C; and Fig. 3, B and C). In contrast, low concentrations of Dox, which provide strong Notch signaling, predominantly induced T cell differentiation, and interestingly, intermediate concentrations of Dox elicited the differentiation of ILC2 and NK/ILC1 (Fig. 2, B and C; and Fig. 3, B and C). Strong Notch signaling also promoted the differentiation of both LTi cells and ILC3 (Fig. 2, D and E; and Fig. 3, D and E). Coculture with both TSt4 Tet-off DLL1 and DLL4 produced similar results (Fig. 2, B–E; and Fig. 3, B–E), suggesting that both DLL1 and DLL4 signaling have the potential to induce ILC differentiation in a dose-dependent manner. We also confirmed the expression of Notch receptors on progenitor populations. Hematopoietic stem cells (HSCs), lymphoid-primed multipotent progenitors, and CLPs express both Notch1 and Notch2, but Notch1 expression disappears after the CHILP stage (Fig. 3 F). Although the strength of Notch signaling seems to

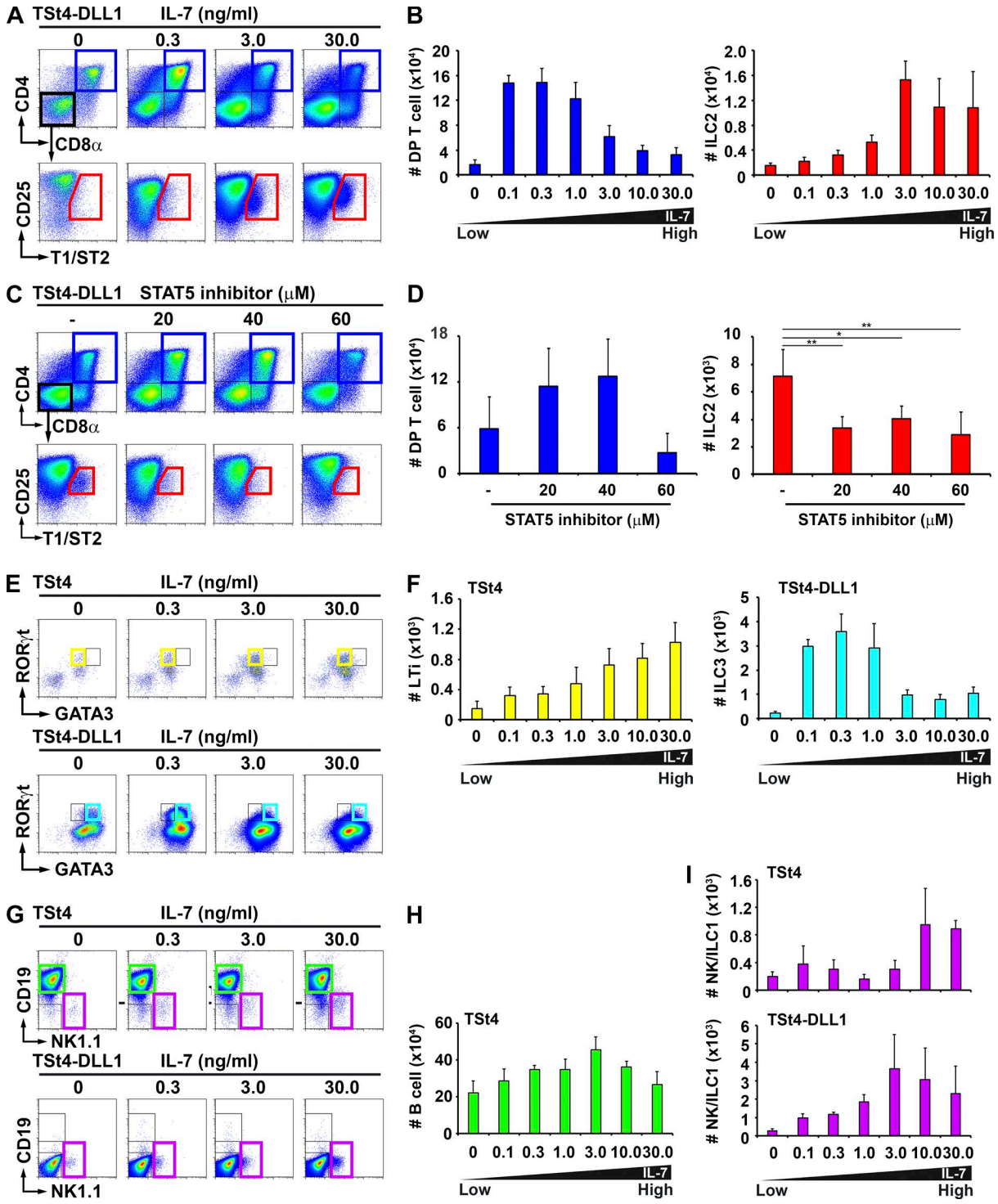

Figure 1. **Lymphocyte cell fate decisions are controlled by IL-7. (A)** Differentiation of DP T cells (blue frame) and ILC2 (red frame) from E15 FL CLP cultured for 10 d in the presence of TSt4-DLL1 stromal cells and different concentrations of IL-7 (0–30 ng/ml). **(B)** Numbers of DP T cells and ILC2 in A. *n* = 3. **(C)** Differentiation of DP T cells (blue frame) and ILC2 (red frame) from CLP cultured for 9 d with TSt4-DLL1 cells in the presence of 10 ng/ml IL-7 and the indicated concentrations of a STAT5 inhibitor. **(D)** Number of DP T cells and ILC2 in C. *n* = 4. **(E)** CLPs were cocultured for 9 d with TSt4 (top) or TSt4-DLL1 (bottom) stromal cells in the presence of the indicated concentrations of IL-7 (0–30 ng/ml). Differentiated cells were then analyzed by flow cytometry. LTi cells are shown as $CD19^-CD4^-CD8\alpha^-ROR\gamma t^+GATA3^{lo}$ (yellow frame) cells, and ILC3 are shown as $CD19^-CD4^-CD8\alpha^-ROR\gamma t^+GATA3^{mid}$ (aqua frame) cells. **(F)** Numbers of LTi/ILC3 in E. *n* = 4. **(G)** CLPs were cocultured with TSt4 (top) or TSt4-DLL1 (bottom) stromal cells and the indicated concentrations of IL-7 (0–30 ng/ml). After 10 d, NK/ILC1 ($CD19^-NK1.1^+$ on TSt4 or TSt4-DLL1 cells; purple frame) and B cells ($CD19^+NK1.1^-$ on TSt4 cells; green frame) were analyzed by flow cytometry. **(H and I)** Number of B cells (H) and NK/ILC1 (I) in G. *n* = 4. Error bars show means ± SD. Results are representative of two independent experiments. *, P < 0.05; **, P < 0.01 (one-way ANOVA with Holm-Sidak post hoc test).

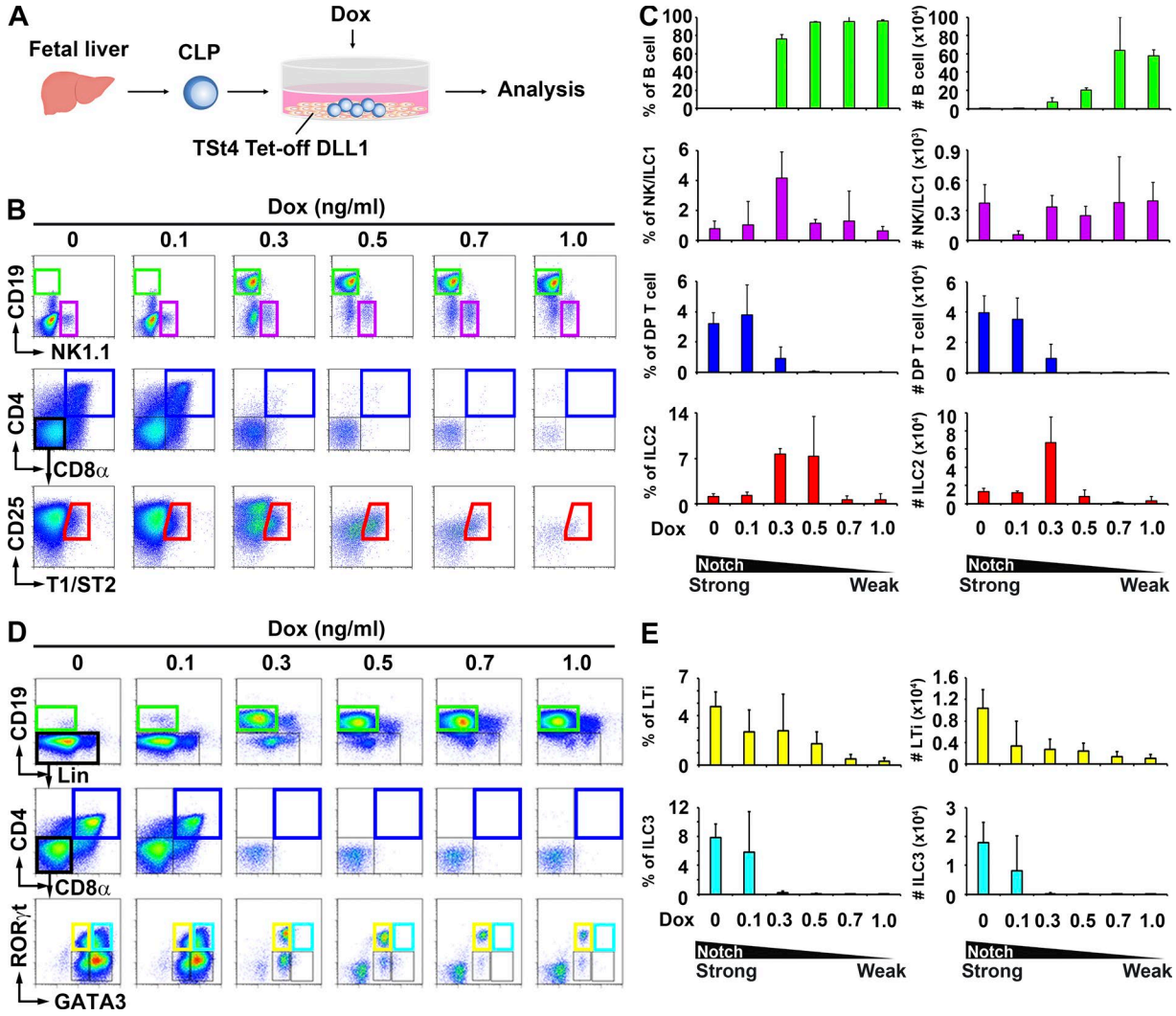

Figure 2. **Different strength of Notch signaling modulates T cell, B cell, and ILC lineage commitment. (A)** Overview of the experimental scheme for the in vitro differentiation of cells isolated from the FL using TSt4 Tet-off DLL1 stromal cells. **(B)** Differentiation of B cells (green frame), NK/ILC1 (purple frame), DP T cells (blue frame), and ILC2 (red frame) from CLP cultured for 10 d with TSt4 Tet-off DLL1 cells in the presence of 10 ng/ml IL-7 and different concentrations of Dox (0–1.0 ng/ml). **(C)** Percentages and numbers of B cells, NK/ILC1, DP T cells, and ILC2 in B. $n = 3$. **(D)** E15 FL CLP were cultured for 10 d with TSt4 Tet-off DLL1 stromal cells, 0.3 ng/ml IL-7, and the indicated concentrations of Dox (0–1.0 ng/ml). Differentiated cells were then analyzed by flow cytometry. LTi cells are shown as RORγt$^+$GATA3^{lo} (yellow frame) cells, and ILC3 are shown as RORγt$^+$GATA3^{mid} (aqua frame) cells. **(E)** The number of LTi/ILC3 in D. $n = 4$. Error bars show means ± SD. Results are representative of two independent experiments.

affect lymphocyte development in the CLP stage in the FL, further experiments are necessary to determine which Notch–DLL interaction is essential for ILC lineage commitment. To confirm whether both IL-7 and Notch signaling cooperatively regulate lymphocyte lineage differentiation, CLPs were cocultured with TSt4 Tet-off DLL1 under different concentrations of IL-7 and Dox. The differentiation of each type of lymphocyte lineage was observed much more clearly when we simultaneously controlled both the concentration of IL-7 and Notch signal strength (Fig. 4, A and B).

Lymphocyte commitment depends on the duration of Notch signaling

We next assessed the effect of the duration of Notch signaling on lymphocyte commitment by adding a high concentration of Dox at different time points (day 1–9) during the coculture of CLP and TSt4 Tet-off DLL1 cells (Fig. 5 A). The presence of Dox from the initiation of coculture (days 0–1 of coculture) predominantly induced B cell differentiation (Fig. 5, B and C). In contrast, when Dox was added later (days 7–8 of coculture), CLP differentiated predominantly into T cells (Fig. 5, B and C). The differentiation of ILC2 and NK/ILC1 was clearly observed when Dox was added on days 2–4 of coculture (Fig. 5, B and C). The differentiation of both LTi cells and ILC3 was enhanced by a longer duration of Notch signaling, which also favors T cell differentiation (Fig. 5, D and E). Similar results were obtained using TSt4 Tet-off DLL4 stromal cells (Fig. S1, A–D). Our data collectively demonstrate that the concentration of IL-7 combined with the strength and duration of Notch signaling determine CLP commitment to the lymphocyte lineage.

CLPs are thought to comprise a heterogeneous population (Mansson et al., 2010) of cell types, including T- and B-committed

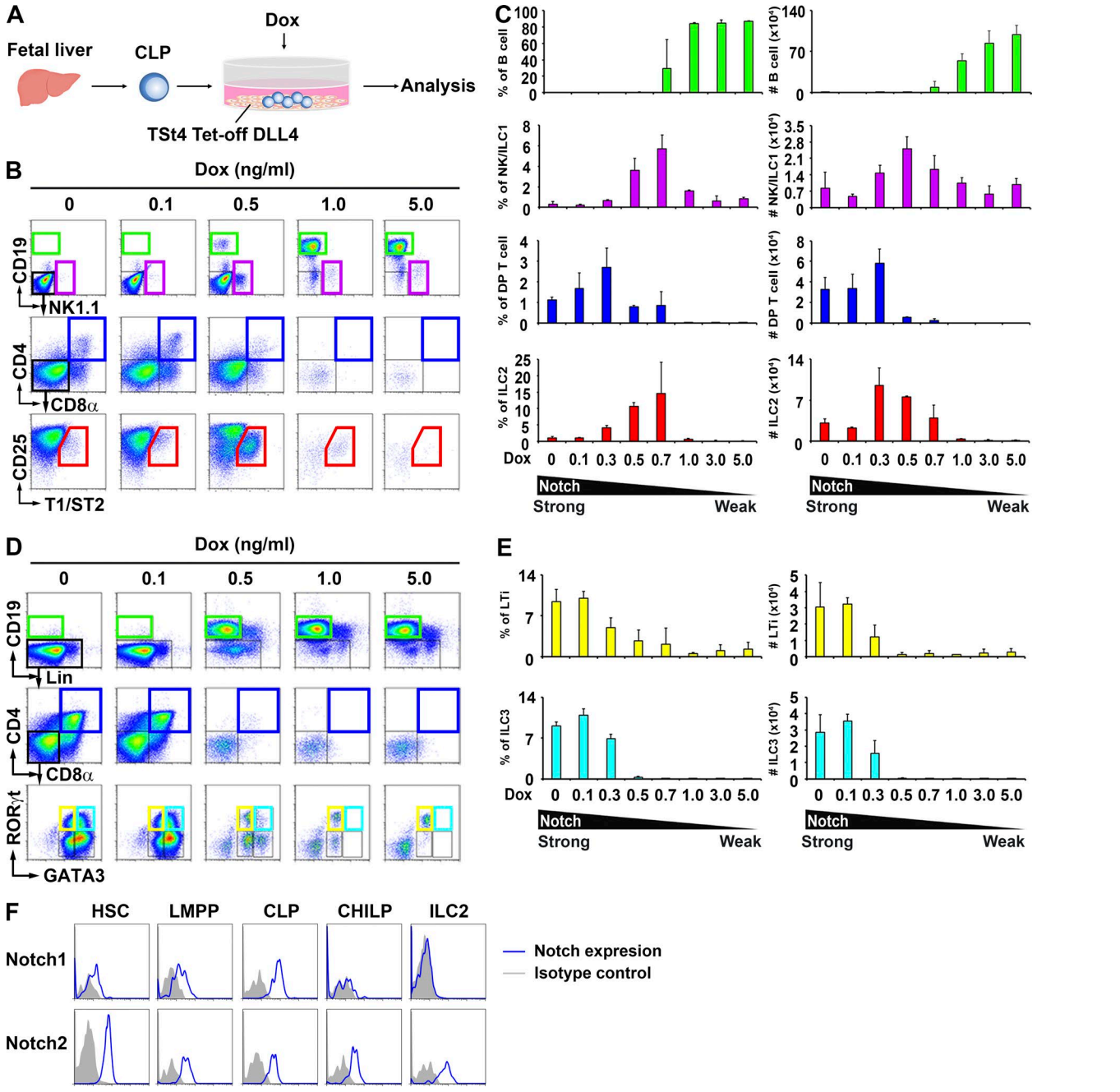

Figure 3. **The differentiation of CLP cultured with TSt4 Tet-off DLL4 cells into distinct types of lymphocytes is dependent on the strength of Notch signaling. (A)** Overview of the experimental scheme for the in vitro differentiation of cells isolated from the FL using TSt4 Tet-off DLL4 stromal cells. **(B)** Differentiation of B cells (green frame), NK/ILC1 (purple frame), DP T cells (blue frame), and ILC2 (red frame) from CLP cultured for 10 d with TSt4 Tet-off DLL1 cells in the presence of 10 ng/ml IL-7 and different concentrations of Dox (0–1.0 ng/ml). **(C)** Percentages and numbers of B cells, NK/ILC1, DP T cells, and ILC2 in B. $n = 3$. **(D)** E15 FL CLP were cultured for 10 d with TSt4 Tet-off DLL4 stromal cells, 0.3 ng/ml IL-7, and the indicated concentrations of Dox (0–1.0 ng/ml). Differentiated LTi/ILC3 were then analyzed by flow cytometry. **(E)** The number of LTi/ILC3 in D. $n = 4$. Error bars show means ± SD. Results are representative of two independent experiments. **(F)** Notch1 and Notch2 expression in various cell populations determined by flow-cytometric analysis. HSCs and lymphoid-primed multipotent progenitor (LMPP) are shown as Lin⁻Sca-1^{hi}c-Kit⁺Flt3⁻IL-7Rα⁻ cells and Lin⁻Sca-1^{hi}c-Kit⁺Flt3⁺IL-7Rα⁻ cells, respectively. Gating strategies for CLP and CHILP are shown in Fig. S2.

progenitors with myeloid potential (Masuda et al., 2005). It is thus possible that the CLP fraction contains ILC2-committed progenitors. In fact, α4β7⁺ ILCPs in the FL have been shown to be a heterogeneous population in a single cell-based analysis (Ishizuka et al., 2016). However, the Lin⁻c-Kit⁺IL-7Rα⁺Flt3⁺ CLP fraction used in this study did not contain the Lin⁻c-Kit⁺IL-7Rα⁺⁻Flt3⁻ CHILP population that can differentiate into all ILC subsets (Fig. S2). We also confirmed that these CLPs did not express α4β7 (unpublished data). Thus, ILC-committed progenitors were not present in the CLP fraction used in this study.

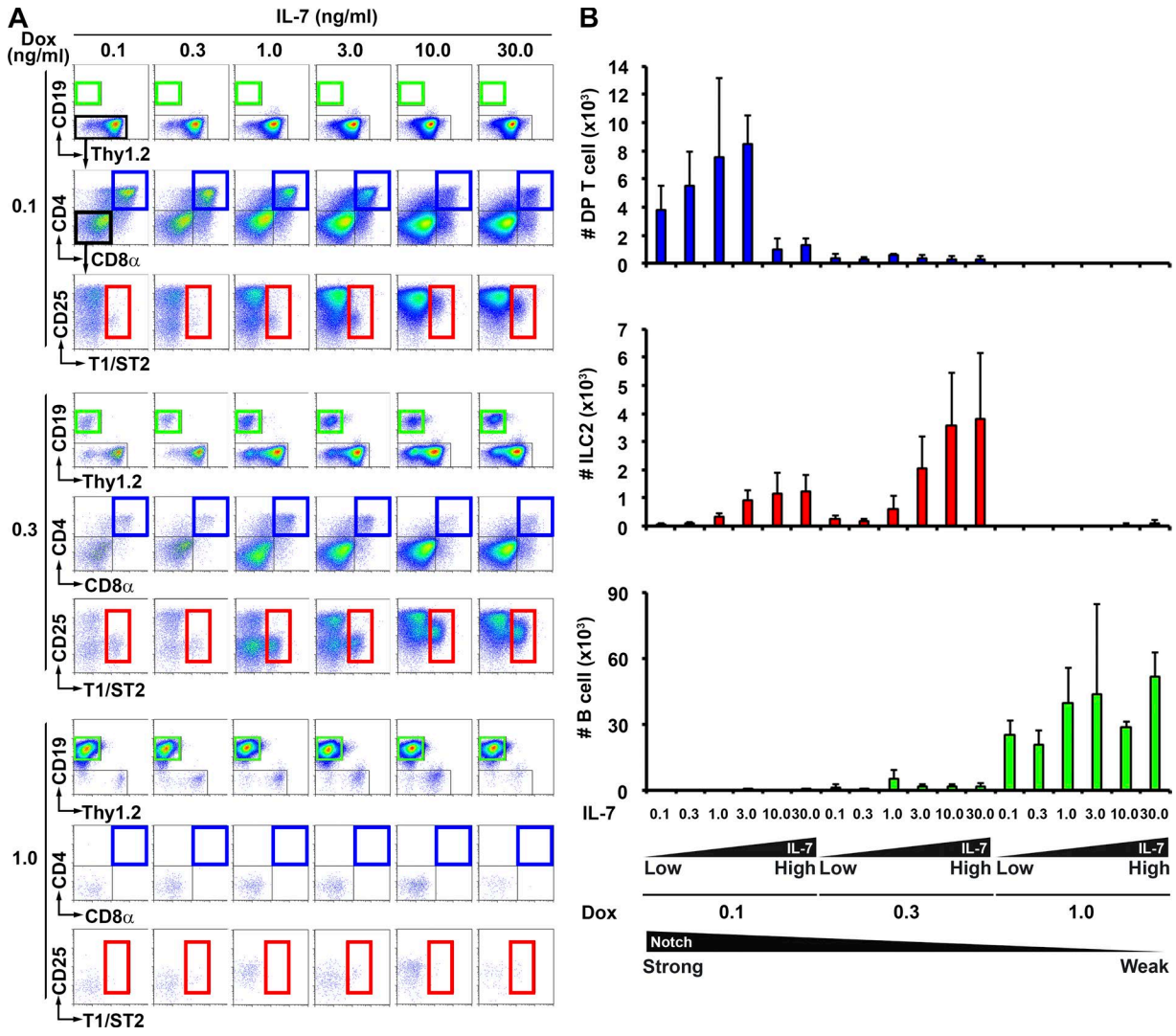

Figure 4. **IL-7 concentration combined with Notch signal strength determine lymphocyte cell fate. (A)** Differentiation of B cells (green frame), T cells (blue frame), and ILC2 (red frame) from E15 FL CLP cultured with TSt4 Tet-off DLL1 cells in the presence of the indicated concentrations of IL-7 (0–30 ng/ml) and Dox (0.1–1.0 ng/ml). Cells were cultured for 9 d and then analyzed by flow cytometry. **(B)** Number of B cells, DP T cells, and ILC2 in A. *n* = 3. Error bars show means ± SD. Results are representative of three independent experiments.

Deletion of DLL4 on thymic epithelial cells induces abnormal expansion of ILC2 in the thymus

To determine the importance of Notch signaling for commitment to T cell and ILC2 differentiation in vivo, we examined the thymus of *FoxN1-Cre-Dll4*$^{flox/flox}$ mice, which lack DLL4 expression on thymic epithelial cells. As expected, T cell development was impaired in these mice (Fig. 6, A and B). However, we observed substantial numbers of both B cells and GATA3$^+$ ILC2s (Fig. 6, A–C). The GATA3$^+$ ILC2s were capable of producing IL-5 and IL-13 in response to IL-2 + IL-25, IL-33, and IL-7 + IL-33, but not IL-25 alone (Fig. 6 D), which are the typical ILC2 cytokine responses. DLL4 is expressed at high levels on not only epithelial cells (FoxN1$^+$ cells) but also nonepithelial cells (FoxN1$^-$ cells), including fibroblasts and endothelial cells in the thymus. It is thus likely that thymocytes in *FoxN1-Cre-Dll4*$^{flox/flox}$ mice were exposed to weak Notch signaling, resulting in differentiation to B cells and ILC2 but not T cells. These results indicate that the extent and magnitude of Notch signaling play a crucial role in the differentiation of ILC2 in vivo as well.

KLRG1$^-$ immature ILC2s exist in the fetal mesentery

Parabiosis studies have suggested that ILC2s are derived from CLPs in the FL but not adult BM in normal, healthy mice, leading to a question about the site of ILC2 differentiation after the FL stage. We therefore focused on the differentiation of ILC2s in the mesentery during the fetal stage because the mesentery contains a large number of ILC2s (Moro et al., 2010). We observed a GATA3$^+$ ILC2 population expressing IL-7Rα and IL-33R (T1/ST2) as early as E15 (Fig. 7 A and not depicted). Compared with ILC2 in the adult mesentery, ILC2 in the fetal mesentery expressed higher levels of c-Kit and lower levels of Sca-1 and Thy1.2 and were negative for KLRG1, a maturation marker for ILC2 and NK cells (Fig. 7 B; Robbins et al., 2002; Huntington et al., 2007). Although adult ILC2s proliferated and produced IL-5 and IL-13 in response to a combination of IL-2 + IL-25 or IL-33 (Moro et al., 2010), fetal ILC2s were insensitive to IL-33 (Fig. 7 C), and acquired IL-33 responsiveness after birth (Fig. 7 D). Interestingly, fetal ILC2s proliferated and produced IL-5 and IL-13 in response

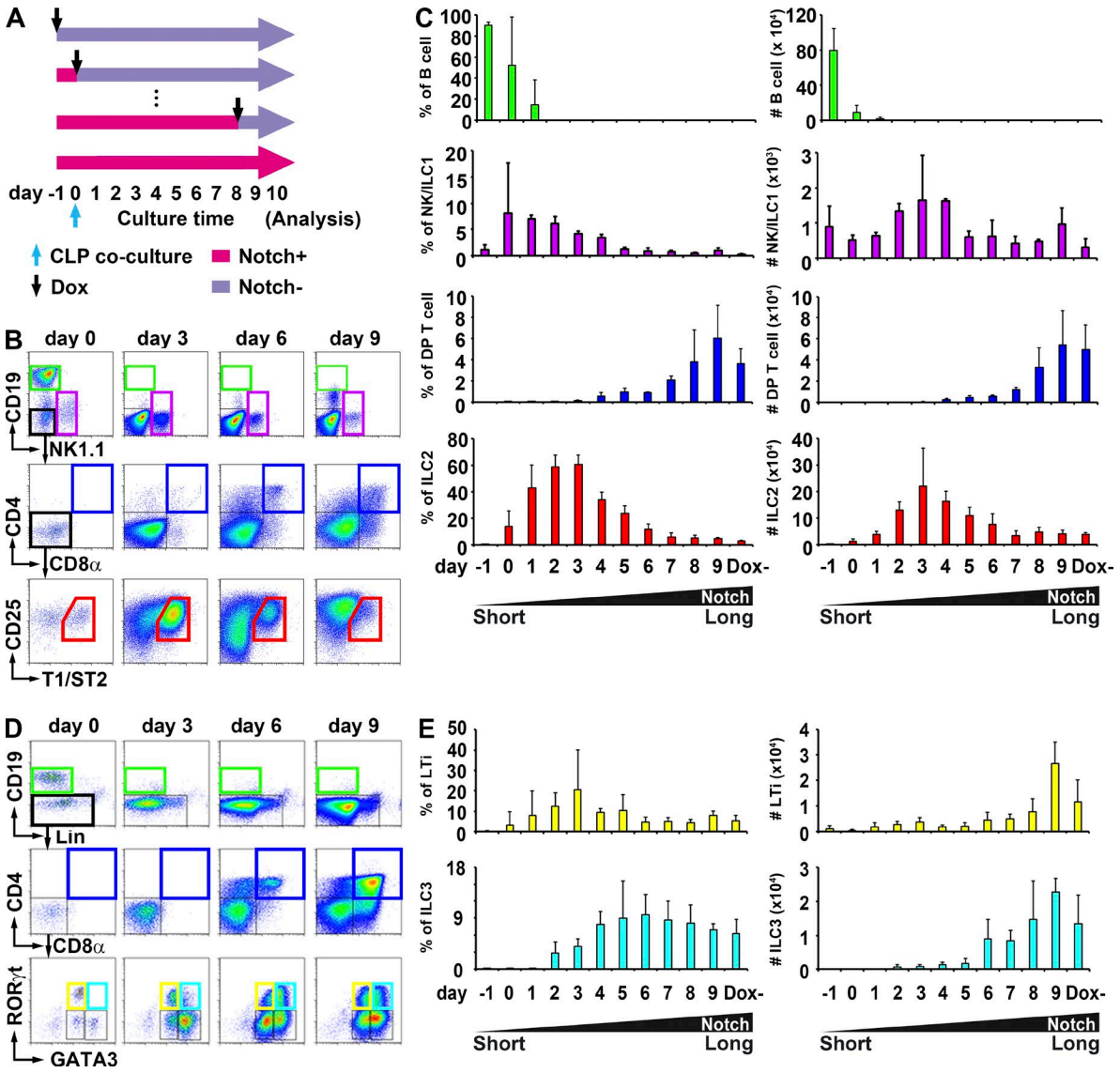

Figure 5. **The duration of Notch signaling determines the differentiation of T cells, B cells, and ILCs. (A)** Flow chart of the experiments performed to investigate the effects of varying the duration of Notch signaling. E15 FL CLPs were cocultured with TSt4 Tet-off DLL1, and Dox was added on day 1, 0, 1, 2, 3, 4, 5, 6, 7, 8, or 9. All samples were analyzed on day 10. **(B)** Differentiation of B cells (green frame), NK/ILC1 (purple frame), DP T cells (blue frame), and ILC2 (red frame) from CLP cultured with TSt4 Tet-off DLL1 cells. Then, 1.0 ng/ml Dox was added on different days, and 10 ng/ml IL-7 was added from day 0 to day 10. Panels are shown for the indicated days. **(C)** Percentages and cell numbers from B. *n* = 4 Results are representative of three independent experiments. **(D)** E15 FL CLPs were cultured with TSt4 Tet-off DLL1 stromal cells. Dox (1.0 ng/ml) was added on the indicated days, and 0.3 ng/ml IL-7 was added from day 0 to day 10. After 10 d, differentiated LTi/ILC3 were analyzed by flow cytometry. **(E)** Numbers of LTi/ILC3 in D. *n* = 4. Error bars show means ± SD. Results are representative of two independent experiments.

to IL-33 in combination with STAT5 activators such as IL-2, IL-7, and TSLP (Fig. 7 E), positive regulators for ILC2 functions (Mjösberg et al., 2012; Kabata et al., 2013). These results suggest that the STAT5 pathway is involved in the maturation of ILC2 and that ILC2s undergo maturation in vivo in the peripheral tissue.

ILCPs and immature ILCs exist in the fetal periphery

Unlike most CD45$^+$Lin$^-$ cells in the adult mesentery, which are mature IL-7Rα$^+$T1/ST2$^+$ ILC2s (Fig. 8 A, red frame), large numbers of CD45$^+$Lin$^-$ cells in the fetal mesentery express IL-7Rα but not T1/ST2 (Fig. 8 A, blue frame). These Lin$^-$IL-7Rα$^+$T1/ST2$^-$ cells in the fetal mesentery express α4β7 and low levels of CD25 and are negative for Flt3 (Fig. 8 B and not depicted). These characteristics are similar to those of CHILP or ILCP in the BM and FL (Constantinides et al., 2014; Klose et al., 2014). Interestingly, the majority of Lin$^-$IL-7Rα$^+$T1/ST2$^-$ cells were RORγt$^+$PLZF^{lo}GATA3^{lo}T-bet$^-$, and only a small number of RORγt$^-$PLZF^{hi}GATA3^{hi}T-bet$^-$ or RORγt$^-$GATA3^{lo}T-bet$^+$ cells were present (Fig. 8 C). Although RORγt$^+$PLZF^{lo}GATA3^{lo}T-bet$^-$ cells comprised a dominant population in the fetal mesentery, their numbers were drastically reduced in the adult mesentery (Fig. 8 D). Lin$^-$IL-7Rα$^+$T1/ST2$^-$ cells in the fetal mesentery could be divided into four populations based on RORγt and CCR9 expression (Fig. 8 E). None of these four populations produced IFNγ, but RORγt$^+$CCR9$^-$ cells had the potential to produce low levels of IL-17A (Fig. 8 F). RORγt$^+$CCR9$^+$, RORγt$^-$CCR9$^+$, and RORγt$^-$CCR9$^-$ cells were IL-13$^{low/-}$ cells

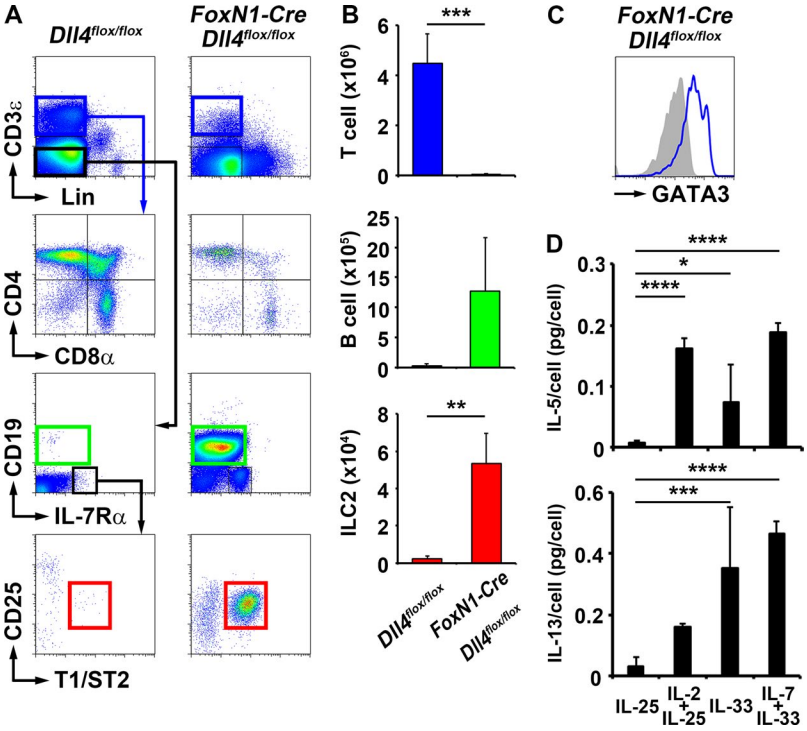

Figure 6. **GATA3⁺ ILC2 development in the thymus of *FoxN1-Cre-Dll4*$^{flox/flox}$ mice. (A)** T cells (blue frame), ILC2 (red frame), and B cells (green frame) in the thymus of *Dll4*$^{flox/flox}$ or *FoxN1-Cre-Dll4*$^{flox/flox}$ mice. **(B)** Numbers of T cells, B cells, and ILC2 in the thymus of mice in A. $n = 2–5$. Results are representative of three independent experiments. **(C)** GATA3 expression in ILC2 in A was analyzed by flow cytometry with anti-GATA3 mAb (blue line) or an isotype-matched control antibody (filled gray line). **(D)** ILC2 from the thymus of *FoxN1-Cre-Dll4*$^{flox/flox}$ mice were isolated and stimulated (3,000 cells/well) with IL-25, IL-2 + IL-25, IL-33, or IL-7 + IL-33 (10 ng/ml each) for 6 d. Production of IL-5 and IL-13 in the supernatants was measured by ELISA. The amounts of cytokines produced are presented as the amounts of cytokine (pg) produced by a single cell. $n = 5$. Error bars show means ± SD *, $P < 0.05$; **, $P < 0.01$; ***, $P < 0.001$; ****, $P < 0.0001$ (Student's *t* test or one-way ANOVA with Holm-Sidak post hoc test).

(Fig. 8 F), suggesting that Lin⁻IL-7Rα⁺T1/ST2⁻ cells contain immature ILCs. When we cocultured the CCR9⁻ or CCR9⁺ fraction of Lin⁻IL-7Rα⁺T1/ST2⁻ cells with TSt4-DLL1 (Fig. 8 G), T-bet⁺ ILC1s (Fig. 8 H, pink frame), GATA3⁺ ILC2s (Fig. 8 H, red frame), and RORγt⁺ ILC3s (Fig. 8 H, blue frame) but not T cells or B cells were observed (not depicted), indicating that the Lin⁻IL-7Rα⁺T1/ST2⁻ fraction contains committed ILCP. The CCR9⁻ fraction dominantly differentiated to ILC1s and ILC3s, but the CCR9⁺ fraction expressed both GATA3 and PLZF (not depicted) and preferentially differentiated to ILC2s (Fig. 8, H and I), suggesting that Lin⁻IL-7Rα⁺T1/ST2⁻CCR9⁺ cells are committed to ILC2. The CCR9⁻ fraction could be divided into RORγt⁺ and RORγt⁻ cells (Fig. 8 E). Although RORγt⁺CCR9⁻ cells seemed to be immature ILC3s based on their IL-17A expression (Fig. 8 F), it is likely that RORγt⁻CCR9⁻ cells were ILCPs. To confirm this possibility, RORγt⁻CCR9⁻ cells from *RORγt*$^{GFP/+}$ mice were sorted and cocultured with TSt4-DLL1. After 10 d, RORγt⁻CCR9⁻ cells had differentiated into all ILCs, including ILC1s (Fig. 8 J, pink frame), ILC2s (Fig. 8 J, red frame), and ILC3s (Fig. 8 J, blue frame). These data collectively indicate that Lin⁻IL-7Rα⁺T1/ST2⁻ cells are heterogeneous populations that include ILC-committed progenitors and immature ILCs. Similar ILCP populations and immature ILC2s requiring STAT5 stimulation for maturation were also detected in the fetal intestine and lung (Fig. S3, A and B). It is likely that CLPs differentiate into CHILP/ILCP in the FL, and CHILP/ILCP then migrate to the peripheral tissues and change their phenotype to Lin⁻IL-7Rα⁺T1/ST2⁻ cells. Our data suggest that CCR9⁺ cells in the Lin⁻IL-7Rα⁺T1/ST2⁻ fraction are ILC2-committed cells, and it is possible that they arise from the CCR9⁻ population in the mesentery.

CD45⁻CD31⁻ stromal cells support ILC2 differentiation

Tissue-specific stromal cells in the thymus or BM control T or B cell development, respectively, demonstrating the importance of stromal cells in the differentiation of lymphocytes. However, which stromal cells, if any, support ILC2 differentiation in vivo is as yet unknown. To identify these stromal cells, total mesenteric cells were isolated, and single-cell RNA-sequence (scRNA-Seq) analysis was performed. Mesenteric cells were divided into 20 clusters based on a two-dimensional *t*-distributed stochastic neighbor embedding projection on duplicate samples (Fig. 9 A). We found two clusters (C16 and C17) that express *Gata3* (GATA3), the first of which did not express *Cd3e* (CD3ε), suggesting that cluster 16 is the likely candidate of the ILC2 cluster (Fig. 9 B). We also found clusters that did not express *Ptprc* (CD45; i.e., nonimmune cells) that are candidates for stromal cells: fraction 1 (F1, containing C2 to C4), fraction 2 (F2, containing C6 to C9), and C5. Specifically, cells in F1 expressed *Pecam1* (CD31), which is a general marker for endothelial cells (Fig. 9 C). By flow-cytometric analysis, mesentery cells were separated into four populations based on their CD45 and CD31 expression, namely CD45^{hi}CD31⁻ (CD45^{hi}), CD45^{lo}CD31⁻ (CD45^{lo}), CD45⁻CD31⁻ (CD45⁻), and CD45⁻CD31⁺ (CD31⁺; Fig. 9 D). To determine the potential of each population to support ILC2 differentiation, we cocultured Lin⁻IL-7Rα⁺T1/ST2⁻ ILCP from the fetal mesentery of WT mice with these four mesenteric populations from *Il2rg*$^{-/-}$*Rag2*$^{-/-}$ mice to eliminate lymphocyte contamination. All samples, with or without stromal cells, displayed low numbers of T-bet⁺ cells and abundant RORγt⁺ cells (Fig. 9, E and F). GATA3⁺ ILC2s were observed only in cocultures containing CD45⁻CD31⁻ cells (Fig. 9, E and F), suggesting that the differentiation of ILC2 is supported by the C5 or F2 population.

CD45⁻CD31⁻PDGFRα⁺gp38⁺ mesenchymal cells support ILC2 differentiation and maturation

We next aimed to identify cluster-specific surface markers to enable separation of the C5 and F2 populations by flow-cytometric

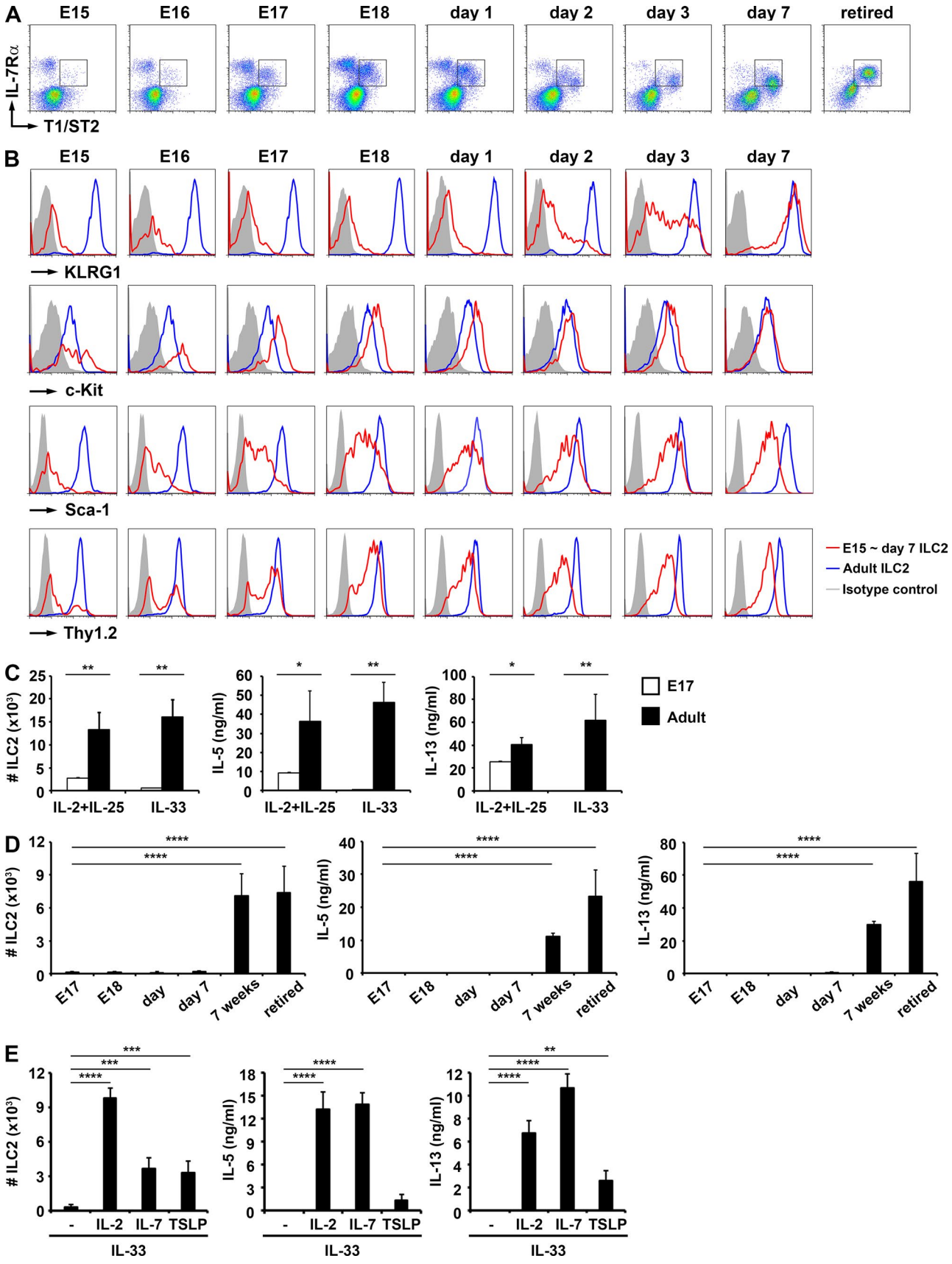

Figure 7. **Immature KLRG1⁻ ILC2 are present in the fetal mesentery. (A)** ILC2 in the mesentery of mice of the indicated ages. Rectangles indicate ILC2. Data were combined from six experiments. **(B)** Expression of KLRG1, c-Kit, Sca-1, and Thy1.2 (red lines) on ILC2 isolated from the mesentery of mice of the indicated embryonic ages. Data from adult mice are shown as blue lines, and isotype-matched control antibodies are shown as filled gray lines. These cells are the same

analysis. Based on the scRNA-Seq data, we first determined that *Pdpn* (gp38), which is a lymphatic endothelial cell marker known to be expressed by IL-33–expressing cells in adipose tissue (Jackson-Jones et al., 2016), was specific to C5 and F2 cells (Fig. 10, A and B). Furthermore, we identified *Pdgfra* (PDGFRα), which is a specific marker for adipocyte precursors and mesenchymal cells (Lee et al., 2012), to be specific to F2 cells (Fig. 10, A and B). Therefore, using gp38 and PDGFRα, the CD45$^-$CD31$^-$ fraction could be further subdivided into three fractions: PDGFRα$^+$gp38$^+$ (PDGFRα$^+$), PDGFRα$^-$gp38^{hi} (gp38^{hi}), and PDGFRα$^-$gp38$^-$ (double negative [DN]; Fig. 10 C). Lin$^-$IL-7Rα$^+$T1/ST2$^-$ ILCPs from the fetal mesentery were cocultured with these subpopulations from *Il2rg*$^{-/-}$*Rag2*$^{-/-}$ mice, and we found that GATA3$^+$ ILC2 differentiation was specifically induced through the support of PDGFRα$^+$ cells (Fig. 10, D and E). Similar results were observed in cocultures using fetal PDGFRα$^+$ cells derived from WT mice (Fig. S4, A–C).

When we examined the gene expression of the four clusters in F2 (Fig. 9 A), 196, 81, 32, and 44 genes were specifically expressed in C6, C7, C8, and C9 clusters, respectively (Fig. 10 F). Among these genes, *Cxcl12* (CXCL12) was highly expressed in C9, which is a critical factor for B cell differentiation and is provided by CXCL12-abundant reticular cells in the BM. A fraction of PDGFRα$^+$ cells in the adult mesentery expressed CXCL12 as determined by flow-cytometric analysis (Fig. 10 G). However, both CXCL12$^+$PDGFRα$^+$ cells and CXCL12$^-$PDGFRα$^+$ cells supported ILC2 differentiation (unpublished data), indicating that, unlike B cells, CXCL12 is not involved in the differentiation of ILC2. We investigated whether PDGFRα$^+$ cells in the mesentery are capable of supporting ILC2 differentiation from CLP. In coculture experiments, GATA3$^+$ ILC2s were induced from CHILPs but not CLPs, strongly suggesting that CLPs require environmental factors in the FL and that the terminal differentiation of ILC2s from CHILP/ILCP occurs with the support of PDGFRα$^+$ cells in the mesentery (Fig. 10 H). Finally, we determined whether PDGFRα$^+$ cells are also able to support ILC2 maturation. Immature ILC2 in the fetal mesentery were cocultured with three stromal cell fractions in the adult mesentery, and their cytokine production abilities in response to IL-33 alone were assessed as a marker of maturation. As expected, PDGFRα$^+$ cells induced IL-5 and IL-13 production from fetal ILC2s (Fig. 10 I), and interestingly, gp38^{hi} cells also induced cytokine production from fetal ILC2s (Fig. 10 I). ILC2 development occurred even in IL-33–deficient mice, indicating that IL-33 signaling is not necessary for ILC2 development (unpublished data). However, the high expression level of IL-33 in both PDGFRα$^+$ cells and gp38^{hi} cells suggests that IL-33 might be a candidate for an accelerator of ILC2 maturation (Fig. 10 J; Jackson-Jones et al., 2016).

Discussion

It is well-known that IL-7 and Notch signaling are essential for T cell and ILC differentiation. However, it remains poorly understood how IL-7 and Notch signaling control the fate of CLP into T cell and ILC lineages. A previous study showed that the overexpression of Notch intracellular domains in human thymic progenitor cells promotes Lin$^-$CRTH2$^+$ILC2 differentiation (Gentek et al., 2013). However, it has been reported that Notch intracellular domains or constitutive Notch signaling induces T cell differentiation (Cherrier et al., 2012; Chea et al., 2016). These seemingly conflicting backgrounds led us to focus on the quantity of environmental factors. In the first half of this study, we demonstrated that the concentration of IL-7 and strength and duration of Notch signaling differentially regulate the commitment to T cell, B cell, and ILC lineages from CLP. The abundant induction of B cells and ILCs in the thymus of epithelial cell-specific DLL4-deleted mice verified the importance of the quantity of environmental factors during cell fate determination.

The next step was the elucidation of the mechanism for regulation of lymphocyte differentiation by IL-7 and Notch signaling. The expression of NFIL3 and TCF-1 is known to be regulated by IL-7 and Notch signaling, respectively (Yang et al., 2013; Xu et al., 2015), and the balance between Id2 and the E protein family such as E2A and EBF is regulated by Notch signaling (Miyazaki et al., 2017). These facts suggest that the quantity of IL-7 and Notch signaling properly adjust the expression of transcriptional factors for lymphocyte differentiation, which should be examined in future studies.

The site and the source of IL-7 and Notch signaling for ILC2 differentiation remain unclear. Identifying the timing in which the appropriate IL-7 concentration affects the cell fate decision is technically difficult because IL-7 is essential for both development and survival of many cell lineages. The fact that ILCPs in the FL can differentiate into ILCs without Notch signaling in vitro (Constantinides et al., 2014) indicates that appropriate Notch signaling is required for the CLP to ILCP stage but not for the post-ILCP stage in the FL. Therefore, we concluded that the IL-7– and Notch-dependent cell fate decision occurs in the FL, and ILC-committed progenitors, including ILCPs and CHILPs, migrate to the peripheral tissues. IL-7 has been shown to be produced by mesenchymal cells and epithelial cells in several tissues (Hara et al., 2012; Liang et al., 2012), and CD45$^-$EpCAM-1$^-$VCAM-1$^+$ICAM-1$^+$ stromal cells in the FL have been reported to express Notch ligand (Harman et al., 2005). We tried to identify both IL-7–producing cells and Notch ligand–expressing cells in the FL; however, there were too many candidate cell populations, and we could not narrow them down in this study.

In the last half of this study, we focused on ILC2 development in the peripheral tissues and identified three different stages of ILC2. The most immature population of these three stages is ILCPs in the Lin$^-$IL-7Rα$^+$T1/ST2$^-$ fraction that differentiate into all ILCs but not T and B cells. The Lin$^-$IL-7Rα$^+$T1/ST2$^-$ fraction seems to be a heterogeneous population because some of these cells express

as those shown in A. **(C)** Proliferative responses and IL-5 and IL-13 cytokine production in response to addition of IL-2 + IL-25 or IL-33 cytokines (10 ng/ml each) to fetal ILC2 (E17) and adult ILC2. $n = 3$. **(D)** Responses of ILC2 isolated from mice of the indicated ages to IL-33 stimulation measured by proliferation and production of IL-5 and IL-13. Retired indicates mice retired from breeding. $n = 5$. **(E)** Effects of the indicated STAT5-activating cytokines (10 ng/ml each) on IL-33–dependent E17 fetal ILC2 proliferation and IL-5 and IL-13 production. $n = 5$. Error bars show means ± SD. Results are representative of two independent experiments. *, P < 0.05; **, P < 0.01; ***, P < 0.001; ****, P < 0.0001 (Student's *t* test or one-way ANOVA with Holm-Sidak post hoc test).

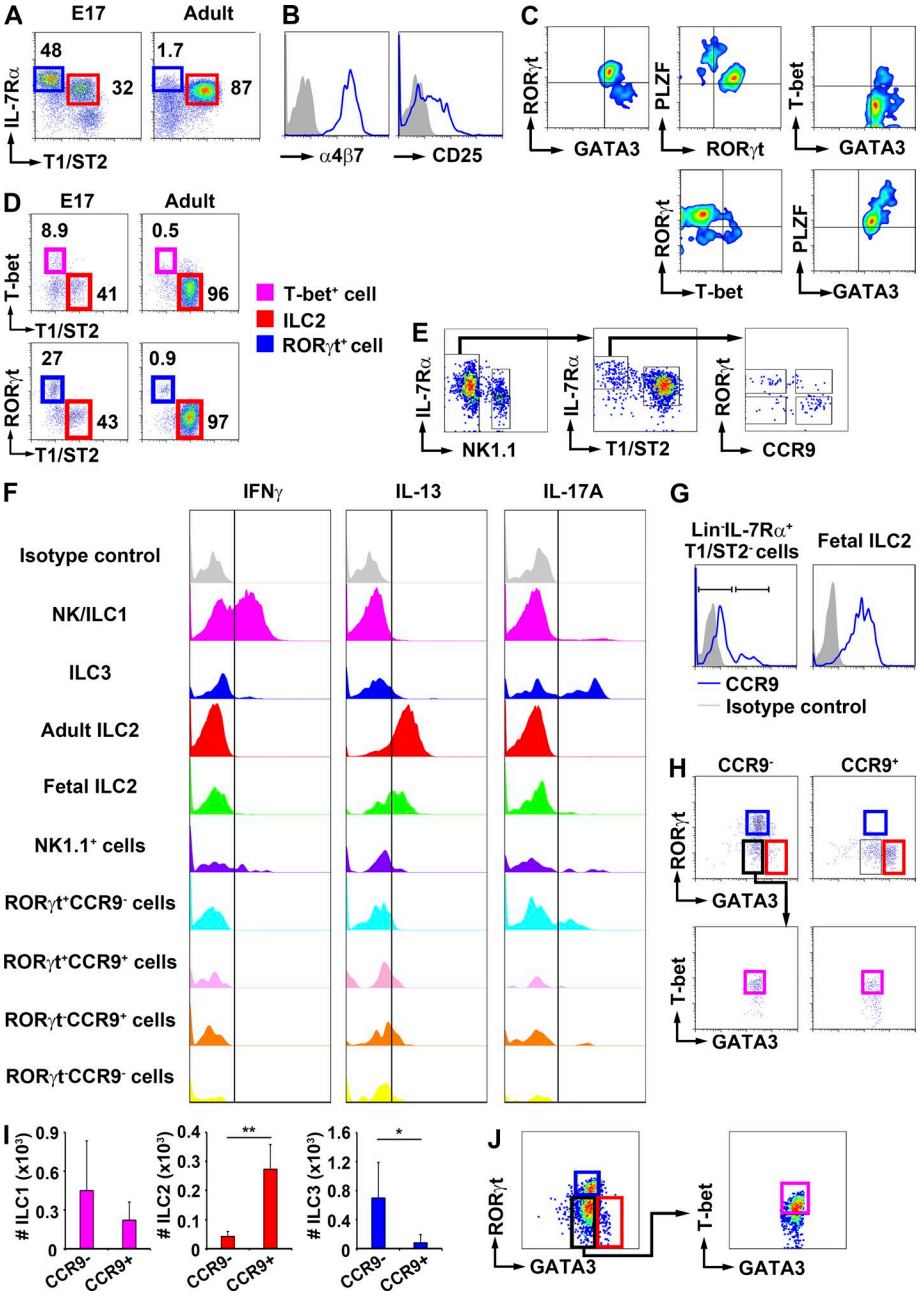

Figure 8. **ILCP, CCR9⁺ ILCP, and immature ILCs exist in the fetal mesentery. (A)** Flow-cytometric analyses of CD45⁺Lin⁻ cells from the E17 fetal or adult mesentery. Numbers indicate the percentage of cells in the boxed areas. **(B and C)** Expression levels of the indicated markers on Lin⁻IL-7Rα⁺T1/ST2⁻ cells from the E17 fetal mesentery. **(D)** Percentages of T-bet⁺ cells (pink frame), RORγt⁺ cells (blue frame), and T-bet⁻RORγt⁻T1/ST2⁺ ILC2 (red frame) in the CD45⁺Lin⁻ fraction of the mesentery from fetal (E17) or adult mice were determined by flow cytometry. **(E)** Flow-cytometric analyses of CD45⁺Lin⁻ cells from the E17 fetal mesentery of *RORγ*$^{GFP/+}$ mice. **(F)** Intracellular cytokine staining of several lymphocytes and progenitors. Whole splenic cells, adult mesenteric cells, and fetal E18 mesenteric cells were stimulated with 50 ng/ml PMA and 1 µg/ml ionomycin and 3 µg/ml brefeldin A solution for 3 h, and the expression levels of IFNγ, IL-13, and IL-17A were analyzed by flow cytometry. NK/ILC1 (Lin⁻NK1.1⁺) and ILC3 (Lin⁻IL-7Rα⁺RORγt⁺) in the spleen, mature ILC2 (Lin⁻NK1.1⁻IL-7Rα⁺T1/ST2⁺) in the adult mesentery, immature ILC2 (Lin⁻NK1.1⁻IL-7Rα⁺T1/ST2⁺) and NK1.1⁺ cells (Lin⁻NK1.1⁺) in the fetal mesentery, and RORγt⁺CCR9⁻ cells, RORγt⁺CCR9⁺ cells, RORγt⁻CCR9⁺ cells, and RORγt⁻CCR9⁻ cells in the Lin⁻NK1.1⁻IL-7Rα⁺T1/ST2⁻ gated cells in the fetal mesentery were assessed. **(G)** CCR9 expression on Lin⁻IL-7Rα⁺T1/ST2⁻ cells and Lin⁻IL-7Rα⁺T1/ST2⁺ fetal ILC2 from the E17 fetal mesentery. **(H)** ILC differentiation from Lin⁻IL-7Rα⁺T1/ST2⁻CCR9⁻ or Lin⁻IL-7Rα⁺T1/ST2⁻CCR9⁺ cells cultured with TSt4-DLL1 and 10 ng/ml IL-7 for 10 d. Blue, red, and pink boxes indicate T-bet⁺ ILC1, GATA3^{hi} ILC2, and RORγt⁺ ILC3, respectively. **(I)** Numbers of ILC1, ILC2, and ILC3 in H. *n* = 4–8. Error bars show means ± SD. **(J)** Lin⁻NK1.1⁻IL-7Rα⁺T1/ST2⁻RORγt⁻CCR9⁻ cells from the E18 fetal mesentery from *RORγt*$^{GFP/+}$ mice were cultured with TSt4-DLL1 cells in the presence of 10 ng/ml IL-7 for 10 d. After 10 d, differentiated cells were assessed for T-bet, GATA3, and RORγt expression by flow cytometry. Blue, red, and pink boxes indicate T-bet⁺ ILC1, GATA3^{hi} ILC2, and RORγt⁺ ILC3, respectively. Results are representative of two independent experiments. *, P < 0.05; **, P < 0.01 (Student's *t* test).

low levels of IL-13 or IL-17A. A specific marker for ILC2 progenitors in the Lin⁻IL-7Rα⁺T1/ST2⁻ fraction is needed to separate these cytokine-expressing cells, and Arginase-1 is a possible candidate (Bando et al., 2015). In the next stage, ILC2 progenitors start expressing CCR9 in the Lin⁻IL-7Rα⁺T1/ST2⁻ fraction and predominantly develop into ILC2s. The role of CCR9 on these progenitors is still unclear, but in the adult mouse, most ILC2s in the BM and small intestine (Hoyler et al., 2012) and a portion of ILC2s in the mesentery (unpublished data) express CCR9. At the final stage, ILC2s become positive for T1/ST2 but, interestingly, are not able to respond to IL-33 alone. We found that IL-33 reactivity is acquired after birth and that STAT5 activators play an important role in this process. There are two possibilities for the source of STAT5 activators. First, ILC2s themselves produce STAT5 activators such as IL-2 and IL-9 after birth. Second, T cells, which are the major source of IL-2, can provide STAT5 signaling for ILC2 after birth.

In this study, we focused on ILCPs in the peripheral tissues but did not investigate them in the adult peripheral tissues. However, c-Kit⁺ ILCPs were reported to exist in adult peripheral tissues such as the lung and gut in a human study (Lim et al., 2017), suggesting that ILC2s are consistently supplied from peripheral tissue–derived ILCPs throughout life. However, the role of ILCPs in the BM remains unclear. several studies have clearly shown that ILC2 development in the BM starts from HSCs and that progenitors gradationally develop into CLPs, EILPs, α–lymphoid progenitors, CHILPs, ILCPs, and ILC2Ps and finally mature ILC2s. We

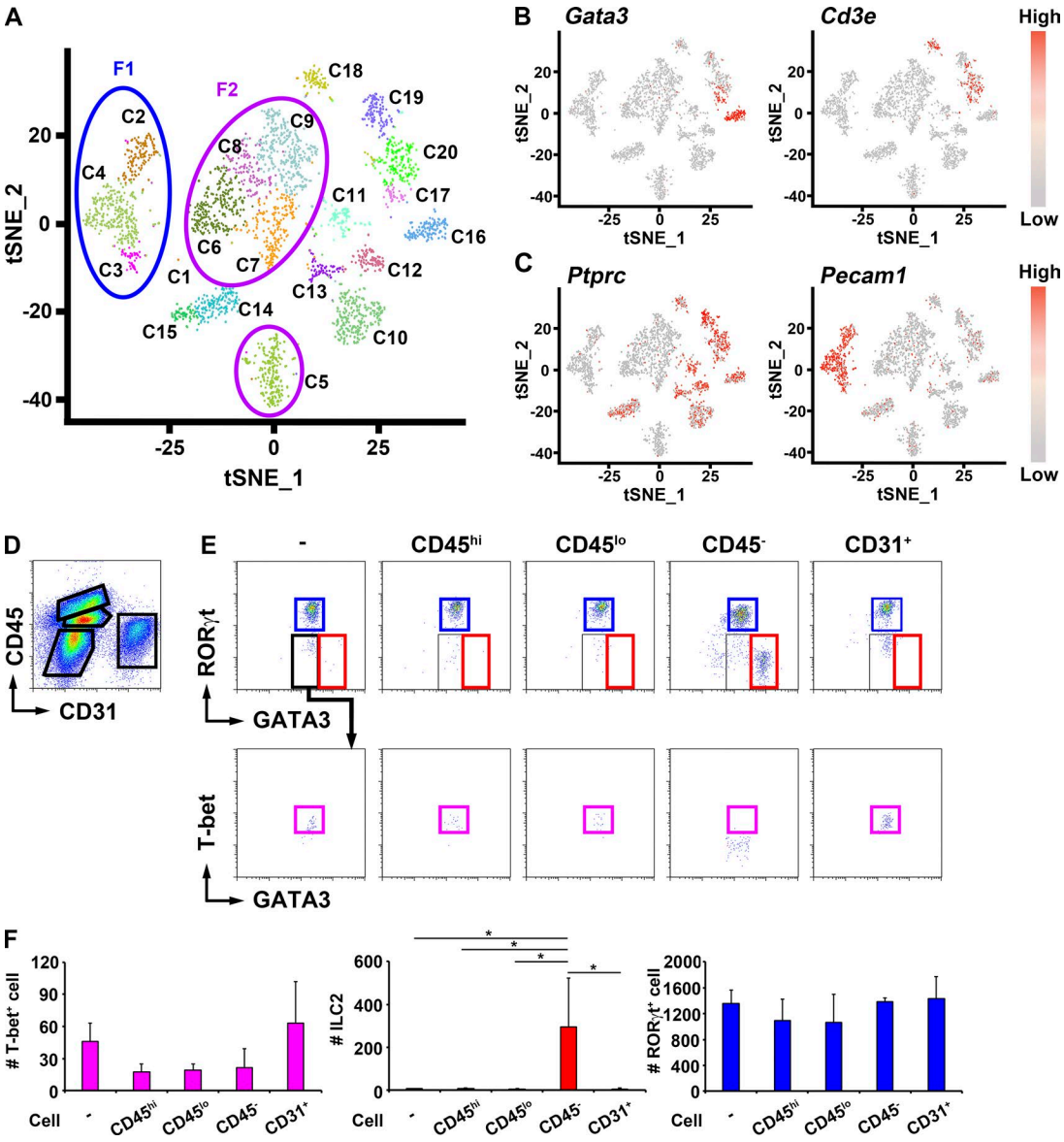

Figure 9. **scRNA-Seq analysis identifies stromal cells that support ILC2 development. (A)** scRNA-Seq analysis of 3,204 total adult mesenteric cells combining two experimental results. Each dot indicates an individual cell. Cells are divided into 20 clusters (Cs) by graph-based clustering. The blue circle indicates F1, and the purple circle indicates F2. **(B and C)** *Gata3* and *Cd3e* (B), *Ptprc*, and *Pecam1* (C) expression within the scRNA-Seq analysis. The density of the red color represents the expression level for each gene. **(D)** Flow-cytometric analysis of cells from the adult mesentery of WT mice for CD45 (*ptprc*) and CD31 (*pecam1*) expression. Results are representative of two independent experiments. **(E)** ILC differentiation from Lin$^-$IL-7Rα$^+$T1/ST2$^-$ ILCP from the E18 fetal mesentery cocultured with CD45$^+$CD31$^-$ (CD45$^+$), CD45^{lo}CD31$^-$ (CD45^{lo}), CD45$^-$CD31$^-$ (CD45$^-$), or CD45$^-$CD31$^+$ (CD31$^+$) cells isolated from the adult mesentery of *Il2rg*$^{-/-}$*Rag2*$^{-/-}$ mice. Cells were cocultured for 10 d in the presence of 10 ng/ml IL-7. Indicated cells are pregated for Lin$^-$ cells. $n = 3$. **(F)** Cell numbers in E. Error bars show means ± SD. Results are representative of two independent experiments. *, $P < 0.05$ (one-way ANOVA with Tukey-Kramer post hoc test). tSNE, *t*-distributed stochastic neighbor embedding.

do not exclude the existence of this process in the BM, but the fact that ILC2s in the parabiosis mouse model did not circulate in the body indicates that progenitors in the BM differentiate into BM-resident ILC2s. It is also possible that BM serves as a reservoir for ILC2s for use in future infections or diseases because a recent study has also reported that ILC2s egress from BM under IL-33 stimulation (Stier et al., 2018). A recent study has shown that EILPs in the BM do not require γ_c-dependent cytokines, including IL-7, for their differentiation (Harly et al., 2018), suggesting that these progenitors are different from FL-derived ILCPs. Many innate type cells such as γδ T cells, B-1 cells, and tissue-resident macrophages are mainly derived from fetal progenitors (Barber et al., 2011; Ghosn et al., 2012; Ramond et al., 2014; Ginhoux and Guilliams, 2016). ILC2s in the peripheral tissue seem to also be derived from fetal progenitors in the steady-state condition.

We identified CD45$^-$CD31$^-$PDGFRα$^+$gp38$^+$ mesenchymal cells in the fetal and adult mesentery as a critical cell population for ILC2 differentiation. A similar population was also identified in the intestine and lung, but the percentage and phenotype were slightly different between each tissue (unpublished data). These results indicate that PDGFRα$^+$gp38$^+$ cells provide an optimal microenvironment for the terminal differentiation of ILC2s in

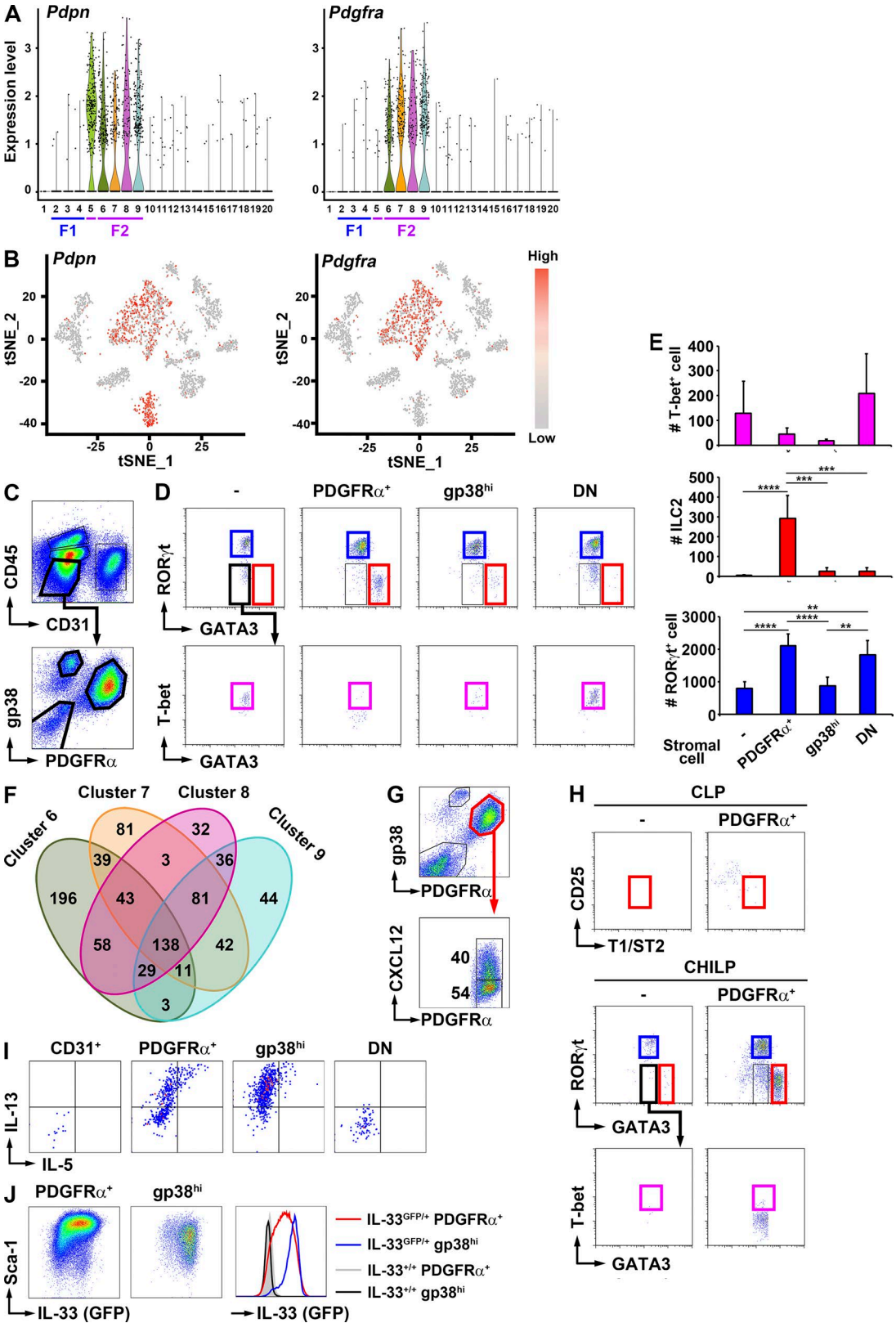

Figure 10. **PDGFRα⁺gp38⁺ mesenchymal cells support ILC2 development in peripheral tissues. (A)** Violin plots of PDGFRα and gp38 expression within the scRNA-Seq clusters shown in Fig. 9 A. The x axis indicates each cluster of F1 and F2, and the y axis indicates the expression level of the indicated gene. **(B)** *Pdpn* (gp38) and *Pdgfra* (PDGFRα) expression within the scRNA-Seq analysis. The density of the red color represents the expression level of the indicated gene. **(C)** Flow-cytometric analysis of WT adult mouse mesentery for gp38 and PDGFRα expression within the CD45 and CD31 DN fraction. **(D)** ILC differentiation from Lin⁻IL-7Rα⁺T1/ST2⁻ ILCP derived from the E18 fetal mesentery and cultured for 10 d in the presence of 10 ng/ml IL-7 and PDGFRα⁺gp38⁺ (PDGFRα⁺), PDG FRα⁻gp38^{hi} (gp38^{hi}), or PDGFRα⁻gp38⁻ (DN) cells isolated from the adult *Il2rg*$^{-/-}$*Rag2*$^{-/-}$ mouse mesentery. Indicated cells are pregated for Lin⁻ cells. **(E)** Cell

each peripheral tissue. PDGFRα⁻gp38^{hi} cells seem to cooperate with PDGFRα⁺gp38⁺ cells to promote the maturation of ILC2s. It will be important to determine the specific factors from each mesenchymal cell population that promote ILC2 differentiation and maturation. Even though IL-7 and Notch signaling play a crucial role in ILC differentiation, PDGFRα⁺gp38⁺ cells do not support ILC2 differentiation from the CLP stage (Fig. 10 H) and do not express *Dll1* (DLL1) and *Dll4* (DLL4) based on scRNA-Seq analysis (not depicted). Unknown factors other than IL-7 and DLL derived from mesenchymal cells are likely involved in ILC2 differentiation from ILCPs. Both PDGFRα⁺gp38⁺ cells and PDGFRα⁻gp38^{hi} cells express IL-33 (Fig. 10 J), and a previous study has demonstrated that IL-33⁺gp38⁺ stromal cells support the activation of ILC2 and B-1 cells in the fat-associated lymphoid cluster (Jackson-Jones et al., 2016), suggesting that IL-33 is involved in the maturation of ILC2s. However, normal ILC2 development can be observed in IL-33–deficient mice, suggesting that IL-33 can be replaced with a different factor. Furthermore, although IL-25 is also an important factor for ILC2 activation, ILC2s are present in IL-25 and IL-33 double-deficient mice (unpublished data), suggesting that IL-25 is not a substitute factor for ILC2 development.

In summary, we conclude that the ILC2 differentiation process consists of two steps: a lineage commitment step in the FL (step 1) and a terminal differentiation step in the peripheral tissues (step 2). During step 1, the concentration of IL-7 together with the strength and duration of Notch signaling coordinately determine the cell fate decision from CLP to CHILP/ILCP in the FL after step 2. In step 2, committed CHILP/ILCP migrate to the fetal peripheral tissues, where CCR9⁺ ILC2-committed ILCPs differentiate into immature ILC2s. During step 2, mesenteric PDGFRα⁺gp38⁺ mesenchymal cells support ILC2 differentiation. Immature ILC2s unable to respond to IL-33 alone undergo functional maturation after birth with the aid of IL-33 or STAT5 signaling from PDGFRα⁺gp38⁺ and PDGFRα⁻gp38^{hi} cells. Our results demonstrate that PDGFRα⁺gp38⁺ mesenchymal cells play a crucial role in ILC2 homeostasis, including differentiation, maturation, and maintenance in the periphery.

Materials and methods

Mice

WT C57BL/6N, retired C57BL/6N, and pregnant C57BL/6J mice were purchased from Charles River Laboratories Japan or CLEA Japan and maintained under specific pathogen-free conditions in the animal facility at the RIKEN Center for Integrative Medical Sciences, Yokohama, Japan. Retired mice are defined as mice older than 4 mo of age that have been retired from breeding. *Il2rg*$^{-/-}$*Rag2*$^{-/-}$ mice (stock 4111) were purchased from Taconic Farms. *FoxN1-Cre* mice were previously described (Hozumi et al., 2008). In brief, the P1 artificial chromosome was used to generate these transgenic mice (clone RPCI21-436p24; Roswell Park Cancer Institute). *FoxN1-Cre-Dll4*$^{flox/flox}$ mice on a mixed background (129/Sv × C57BL/6) were obtained by crossing *FoxN1-Cre* and *Dll-4*$^{flox/flox}$ mice (Hozumi et al., 2008). *CXCL12-GFP* knock-in mice on a C57BL/6 background were previously described (Nagasawa et al., 1996). *RORγt*$^{GFP/+}$ mice on a C57BL/6 background (Eberl et al., 2004) were provided by D. Littman of New York University, New York, NY, and S. Fagarasan of the RIKEN Center for Integrative Medical Sciences. *Il33*$^{GFP/+}$ mice on a C57BL/6 background (Oboki et al., 2010) were provided by S. Nakae (University of Tokyo, Tokyo, Japan). All experiments were approved by the Institutional Animal Care and Use Committees of the RIKEN Center for Integrative Medical Sciences and Tokai University (Tokyo, Japan) and were performed in accordance with institutional guidelines.

Antibodies and reagents

For flow-cytometric analyses, mAbs specific for mouse CD3ε (145-2C11), CD8α (53–6.7), CD19 (1D3), B220 (RA3-6B2), NK1.1 (PK136), CD11b (M1/70), CD11c (HL3), Gr-1 (RB6-8C5), TER119 (TER119), CD45.1 (A20), CD45.2 (2F1), Sca-1 (E13-161.7), CD25 (PC61), Thy1.2 (53–2.1), Flt3 (A2F10), α4β7 (DATK32), KLRG1 (2F1), CCR9 (CW-1.2), CD31 (MEC13.3), GATA3 (L50-823), T-bet (O4-46), RORγt (Q31-378), IFN-γ (XMG1.2), IL-17A (TC11-18H10), and fluorochrome-conjugated streptavidin were purchased from BD. mAbs against mouse Notch1 (HMN1-12), Notch2 (HMN2-35), CD4 (GK1.5), PDGFRα (ATA5), gp38 (8.1.1), and PLZF (9E12) were purchased from BioLegend. mAbs against c-Kit (2B8), FcεRIα (MAR-1), IL-7Rα (A7R34), and IL-13 (eBio13A) were purchased from eBioscience. Anti-T1/ST2 (DJ8) was purchased from MD Biosciences. mAb against mouse CD16/CD32 (2.4G2) was purified from hybridoma culture supernatants in our laboratory.

Recombinant mIL-2, mIL-7, mIL-25, mIL-33, and mTSLP were purchased from R&D Systems. A STAT5 inhibitor (CAS 285986–31-4) was purchased from Calbiochem, and Dox was purchased from Clontech.

Preparation of cell suspensions

FL and thymus samples were mechanically dissociated by passage through 70-µm filters. Cells were suspended in HBSS (Thermo

numbers in D. *n* = 3–8. Data were combined from two experiments. **(F)** Venn diagram of clusters 6 to 9 from the scRNA-Seq analysis in Fig. 9 A. Values were calculated using the differential gene expression levels for each cluster compared with all other cells to give a percent expression value. Only cells with a value over the 0.25 cutoff were retained. The p-value for each gene expression level was calculated using Student's *t* test analysis. The values indicate the numbers of genes highly expressed in each cluster. **(G)** CXCL12 (GFP) expression in PDGFRα⁺gp38⁺ cells from the adult mesentery of *CXCL12-GFP* knock-in mice. Indicated cells are pregated for CD45⁻CD31⁻ cells. **(H)** ILC2 differentiation from CLP or CHILP derived from the E15 FL and cultured for 12 d in the presence of 10 ng/ml IL-7⁻ or IL-7⁺DGFRα⁺gp38⁺ cells (PDGFRα⁺) isolated from WT mouse adult mesentery. Indicated cells are pregated for Lin⁻ cells. **(I)** IL-5 and IL-13 intracellular staining of cells derived from Lin⁻IL-7Rα⁺T1/ST2⁺ immature ILC2 from the E18 fetal mesentery. Immature ILC2 were cultured for 7 d in the presence of 10 ng/ml IL-33 and CD45⁻CD31⁺ (CD31⁺), CD45⁻CD31⁻PDGFRα⁺gp38⁺ (PDGFRα⁺), CD45⁻CD31⁻PDGFRα⁻gp38^{hi} (gp38^{hi}), or CD45⁻CD31⁻PDGFRα⁻gp38⁻ (DN) cells isolated from WT mouse adult mesentery. Indicated cells are pregated for CD45.2⁺ cells. **(J)** IL-33 (GFP) expression of PDGFRα⁺ cells and gp38^{hi} cells isolated from adult *IL-33*$^{GFP/+}$ and *IL-33*$^{+/+}$mice. Histogram (left) showing GFP expression for the indicated cells. Error bars show means ± SD. Results are representative of two independent experiments. *, P < 0.05; **, P < 0.01; ***, P < 0.001; ****, P < 0.0001 (one-way ANOVA with Tukey-Kramer post hoc test). tSNE, *t*-distributed stochastic neighbor embedding.

Fisher Scientific) containing 2% FBS (Japan Bioserum) and 0.1% $NaHCO_3$. Adult ILC2 and stromal cells were isolated from the mesentery as previously described (Moro et al., 2015). To isolate Lin$^-$IL-7Rα$^+$T1/ST2$^-$ cells, ILC2, and stromal cells from the fetal mesentery, fetal mesenteries were harvested using fine-tipped tweezers under a stereomicroscope, and cells were isolated using a method similar to that used for the ILC2 in the adult mesentery. Fetal intestine and lung cells were isolated using Liberase high dispase (Roche) and Liberase thermolysin (Roche), respectively.

Flow-cytometric analysis

Cells were isolated as described above and suspended in HBSS containing 2% FBS and 0.2% sodium azide. Cell suspensions were incubated with 50 µl of purified mAbs against mouse CD16/CD32 (2 µg/ml) and fluorochrome-conjugated antibodies for 20 min on ice. Before flow-cytometric analysis, cells were suspended in 0.5 µg/ml propidium iodide solution to distinguish between live and dead cells. For intracellular staining, cells were fixed and permeabilized with a Foxp3 Staining Set (eBioscience) or IntraPrep Permeabilization Reagent (Beckman Coulter) according to the manufacturer's protocols. Cells were analyzed using a FACSCalibur, FACSAria IIu, or FACSAria III (BD) and sorted using a FACSAria IIu or FACSAria III. All data were analyzed using FlowJo software (TreeStar). Within each experiment, we used several types of lineage markers. To clearly present the gating strategies, the lineage markers and pregating lists are provided in Table S1.

Sorting of progenitors

E15 FL cells were isolated as described above and incubated with 500 µl purified mAb against mouse CD16/CD32 (2 µg/ml) and appropriate concentrations of biotin-conjugated mAbs against CD3ε, B220, CD11b, Gr-1, and TER119 for 20 min. Cells were then washed and incubated with 100–500 µl streptavidin microbeads (Miltenyi Biotec) for 20 min, and lineage-negative cells were enriched using autoMACS (Miltenyi Biotec). For the detection of CLP and CHILP, cells were stained with 500 µl of a solution containing appropriate concentrations of mAbs against Sca-1, c-Kit, IL-7Rα, Flt3, α4β7, and CD25 followed by incubation with 500 µl streptavidin. The gating strategies for Lin$^-$Sca-1^{low}c-Kit$^+$IL-7Rα^{+-}Flt3$^+$ CLP and Lin$^-$c-Kit$^+$IL-7Rα$^+$α4β7$^+$Flt3$^-$CD25$^-$ CHILP are provided in Fig. S2. To sort Lin$^-$IL-7Rα$^+$T1/ST2$^-$ ILCP or ILC2 from the fetal mesentery, E18 fetal mesenteric cells were isolated as described above and stained with mAbs against the lineage markers, T1/ST2, IL-7Rα, and streptavidin.

In vitro differentiation assays

TSt4 and TSt4-DLL1 stromal cells were provided by H. Kawamoto (Kyoto University, Kyoto, Japan) and were described previously (Watanabe et al., 1992; Miyazaki et al., 2005). To establish the TSt4 Tet-off DLL1 and TSt4 Tet-off DLL4 systems, the *DLL1* or *DLL4* gene under the control of a TetO-CMV promoter in a modified TetR expression vector was transfected into TSt4 stromal cells using a lentiviral vector. GFP$^+$ transfected cells were sorted and cultured in 24-well plates for 2 d before the coculture experiments were initiated, and when used, Dox was added 1 d before the initiation of cocultures. FL-derived CLP cells (100 cells) were seeded in the presence of TSt4, TSt4-DLL1, TSt4 Tet-off DLL1, or TSt4 Tet-off DLL4 cells with various IL-7 concentrations or 10 ng/ml IL-7 with various concentrations of Dox for 9–10 d. Fetal mesentery–derived Lin$^-$IL-7Rα$^+$T1/ST2$^-$CCR9$^+$ or Lin$^-$IL-7Rα$^+$T1/ST2$^-$CCR9$^-$ cells (80 cells) and Lin$^-$IL-7Rα$^+$T1/ST2$^-$RORγt$^-$CCR9$^-$ cells (150–500 cells) were cocultured with TSt4 or TSt4-DLL1 cells in the presence of 10 ng/ml IL-7 for 10 d.

FL-derived CLP (100–200 cells), CHILP (200–300 cells), fetal mesentery–derived Lin$^-$IL-7Rα$^+$T1/ST2$^-$ ILCP (150–300 cells), and fetal mesentery–derived Lin$^-$IL-7Rα$^+$T1/ST2$^+$ ILC2 (150–300 cells) were also cocultured with fetal or adult mesentery–derived primary cells (5,000-25,000 cells) in the presence of 10 ng/ml IL-7 for 9–12 d or 10 ng/ml IL-33 for 4–6 d in 96-well flat-bottom plates. Cells were cultured in RPMI-1640 (Sigma-Aldrich) containing 10% FBS (Japan Bioserum), 10 mM Hepes (Sigma-Aldrich), 100 µM nonessential amino acids (Sigma-Aldrich), 1 mM sodium pyruvate (Gibco), 100 U/ml penicillin (Gibco), 100 µg/ml streptomycin (Gibco), and 50 µM 2-mercaptoethanol (Gibco) at 37°C under 5% CO_2.

ILC2 proliferation and cytokine production assays

Purified fetal ILC2 or adult ILC2 from mesenteries and adult ILC2 from thymus were cultured at 500 and 3,000 cells per well, respectively, in 96-well round-bottom plates. The culture medium used was 200 µl RPMI-1640 containing 10% FBS, 10 mM Hepes, 100 µM nonessential amino acids, 1 mM sodium pyruvate, 100 U/ml penicillin, 100 µg/ml streptomycin, and 50 µM 2-mercaptoethanol, and the cells were cultured at 37°C under 5% CO_2. We added 10 ng/ml mIL-2, mIL-7, mTSLP, mIL-25, or mIL-33 to the medium. After 6 d, supernatants were collected, and the amounts of IL-5 and IL-13 were measured using Quantikine ELISA kits or DuoSet ELISA Development kits (R&D Systems) according to the manufacturer's protocols. The total numbers of cells were counted using a hemocytometer. The cytokine production of total cells was expressed as the concentration (ng/ml) and, for a single cell, as the absolute amount (pg cytokine/cell). To determine the potential for cytokine production, cells were cultured at 5×10^5 cells per well in 24-well flat-bottom plates with 50 ng/ml PMA (Sigma-Aldrich), 1 µg/ml ionomycin (Sigma-Aldrich), and 3 µg/ml brefeldin A solution (eBioscience). After 3 h of culture, we collected each cell, performed intracellular staining, and analyzed by flow cytometry.

Single-cell library construction, sequencing, and analyses

Single-cell encapsulation and library construction were performed with the Chromium Controller with the Chromium Single Cell 3′ v2 Reagents kit (10× Genomics) according to the manufacturer's protocols. Cells were loaded onto the Chromium Controller in 10% FCS RPMI Complete medium. Libraries were sequenced on a HiSeq 2,500 instrument (Illumina) and processed with Cell Ranger. An advanced clustering algorithm was performed using Seurat (Satija et al., 2015) on the duplicate samples, which contained 1,516 and 1,679 cells, respectively. Violin plots were generated to determine clear outliers noted by their high gene numbers (unpublished data), which were treated as multiplets and excluded from further analysis. Specifically, cells with 200–3,000 genes with <8,000 total transcripts were selected as single cells. Potential dead cells (cells with >0.5% mitochondrial

genes) were further filtered out. PCA analysis on combined replicates showed very good clustering overlap (unpublished data). Therefore, these were treated as one sample in all other analyses. Highly variable genes were detected using the MeanVarplot command in Seurat. These analyses resulted in 2,475 cells containing at least one highly expressed gene. Twenty PCs were generated from these selected cells and then used to project each individual cell onto a single two-dimensional map using *t*-distributed stochastic neighbor embedding (Macosko et al., 2015), which resulted in 20 distinct clusters. A highly expressed marker specific for each cluster was then identified.

Data accession

The scRNA-Seq data were deposited in NCBI GEO with the accession no. GSE102665.

Statistical analysis

Data presented as the means ± SD were analyzed using Prism 6 (GraphPad Software). A Student's *t* test was used to determine statistically significant differences between two groups. One-way ANOVA with the Holm-Sidak post hoc test or one-way ANOVA with the Tukey-Kramer post hoc test was used to determine statistically significant differences between two or more groups. All reported p-values were calculated using parametric two-tailed tests unless otherwise stated.

Online supplemental material

Fig. S1 shows differentiated T cells, B cells, and ILCs after coculture of CLP with TSt4 and TSt4-DLL4 cells under different durations of Notch signaling. Fig. S2 presents the gating strategy for the detection of CLP and CHILP. Fig. S3 describes distribution and cytokine production of ILCP and ILC2 in the fetal intestine and lung. Fig. S4 presents ILC2 differentiation from Lin$^-$IL-7Rα$^+$T1/ST2$^-$ cells cocultured with PDGFRα$^+$gp38$^+$ mesenchymal cells in the fetal mesentery. Table S1 shows list of lineage markers of each figure.

Acknowledgments

We thank H. Kawamoto, S. Nakae, D. Littman, and S. Fagarasan for providing materials, and we thank T. Ikawa and T. Sugiyama for their technical and scientific advice. We would also like to thank N. Takeno, M. Mochizuki, S. Wada, T. Yamamoto, T. Shitamichi, S. Tada, R. Okuno, Y. Sasako, A. Saito, and N. Hagiwara for technical support and animal care; K.N. Ealey and L.K. Clayton for the critical reading of the manuscript; and other laboratory members for discussions.

This work was supported by a Grant-in-Aid for Japan Society for the Promotion of Science Fellows (14J07705) to S. Koga; a Grant-in-Aid for Scientific Research (26293110) and a Grant-in-Aid for Challenging Exploratory Research (24659373) to K. Moro; Japan Society for the Promotion of Science Grants-in-Aid for Scientific Research (22229004), Scientific Research (16H02631), and Challenging Exploratory Research (25670235) to S. Koyasu; a Precursory Research for Embryonic Science and Technology (PRESTO) grant from the Japan Science and Technology Agency, a Grant-in-Aid for Scientific Research on Innovative Areas from the Ministry of Education, Culture, Sports, Science and Technology (15H01166), a Practical Research Project for Allergic Diseases and Immunology grant from the Japan Agency for Medical Research and Development (16764150), and grants from the Heiwa Nakajima Foundation, the Uehara Memorial Foundation, and the Mochida Memorial Foundation for Medical and Pharmaceutical Research to K. Moro.

The authors declare no competing financial interests.

Author contributions: S. Koga designed and interpreted the experiments and wrote the manuscript; K. Hozumi, K. Hirano, and M. Yazawa prepared DLL1/DLL4 lentiviral vectors and *FoxN1-Cre-Dll4$^{flox/flox}$* mice and assisted with other supporting experiments; T. Terooatea and A. Minoda performed scRNA-Seq; T. Nagasawa prepared *CXCL12-GFP* knock-in mice; S. Koyasu discussed results with S. Koga and wrote the manuscript; and K. Moro supervised all experiments, discussed results with S. Koga, and wrote the manuscript.

Submitted: 19 December 2017
Revised: 5 April 2018
Accepted: 11 April 2018

References

Andrawes, M.B., X. Xu, H. Liu, S.B. Ficarro, J.A. Marto, J.C. Aster, and S.C. Blacklow. 2013. Intrinsic selectivity of Notch 1 for Delta-like 4 over Delta-like 1. *J. Biol. Chem.* 288:25477–25489. https://doi.org/10.1074/jbc.M113.454850

Artis, D., and H. Spits. 2015. The biology of innate lymphoid cells. *Nature.* 517:293–301. https://doi.org/10.1038/nature14189

Bando, J.K., H.E. Liang, and R.M. Locksley. 2015. Identification and distribution of developing innate lymphoid cells in the fetal mouse intestine. *Nat. Immunol.* 16:153–160. https://doi.org/10.1038/ni.3057

Barber, C.L., E. Montecino-Rodriguez, and K. Dorshkind. 2011. Reduced production of B-1-specified common lymphoid progenitors results in diminished potential of adult marrow to generate B-1 cells. *Proc. Natl. Acad. Sci. USA.* 108:13700–13704. https://doi.org/10.1073/pnas.1107172108

Besseyrias, V., E. Fiorini, L.J. Strobl, U. Zimber-Strobl, A. Dumortier, U. Koch, M.L. Arcangeli, S. Ezine, H.R. Macdonald, and F. Radtke. 2007. Hierarchy of Notch-Delta interactions promoting T cell lineage commitment and maturation. *J. Exp. Med.* 204:331–343. https://doi.org/10.1084/jem.20061442

Chea, S., S. Schmutz, C. Berthault, T. Perchet, M. Petit, O. Burlen-Defranoux, A.W. Goldrath, H.R. Rodewald, A. Cumano, and R. Golub. 2016. Single-Cell Gene Expression Analyses Reveal Heterogeneous Responsiveness of Fetal Innate Lymphoid Progenitors to Notch Signaling. *Cell Reports.* 14:1500–1516. https://doi.org/10.1016/j.celrep.2016.01.015

Cherrier, M., S. Sawa, and G. Eberl. 2012. Notch, Id2, and RORγt sequentially orchestrate the fetal development of lymphoid tissue inducer cells. *J. Exp. Med.* 209:729–740. https://doi.org/10.1084/jem.20111594

Clark, M.R., M. Mandal, K. Ochiai, and H. Singh. 2014. Orchestrating B cell lymphopoiesis through interplay of IL-7 receptor and pre-B cell receptor signalling. *Nat. Rev. Immunol.* 14:69–80. https://doi.org/10.1038/nri3570

Constantinides, M.G., B.D. McDonald, P.A. Verhoef, and A. Bendelac. 2014. A committed precursor to innate lymphoid cells. *Nature.* 508:397–401. https://doi.org/10.1038/nature13047

De Obaldia, M.E., and A. Bhandoola. 2015. Transcriptional regulation of innate and adaptive lymphocyte lineages. *Annu. Rev. Immunol.* 33:607–642. https://doi.org/10.1146/annurev-immunol-032414-112032

De Smedt, M., I. Hoebeke, K. Reynvoet, G. Leclercq, and J. Plum. 2005. Different thresholds of Notch signaling bias human precursor cells toward B-, NK-, monocytic/dendritic-, or T-cell lineage in thymus microenvironment. *Blood.* 106:3498–3506. https://doi.org/10.1182/blood-2005-02-0496

Ealey, K.N., K. Moro, and S. Koyasu. 2017. Are ILC2s Jekyll and Hyde in airway inflammation? *Immunol. Rev.* 278:207–218.

Eberl, G., S. Marmon, M.J. Sunshine, P.D. Rennert, Y. Choi, and D.R. Littman. 2004. An essential function for the nuclear receptor RORgamma(t) in the generation of fetal lymphoid tissue inducer cells. *Nat. Immunol.* 5:64–73. https://doi.org/10.1038/ni1022

Gasteiger, G., X. Fan, S. Dikiy, S.Y. Lee, and A.Y. Rudensky. 2015. Tissue residency of innate lymphoid cells in lymphoid and nonlymphoid organs. *Science.* 350:981–985. https://doi.org/10.1126/science.aac9593

Gentek, R., J.M. Munneke, C. Helbig, B. Blom, M.D. Hazenberg, H. Spits, and D. Amsen. 2013. Modulation of Signal Strength Switches Notch from an Inducer of T Cells to an Inducer of ILC2. *Front. Immunol.* 4:334. https://doi.org/10.3389/fimmu.2013.00334

Ghosn, E.E., R. Yamamoto, S. Hamanaka, Y. Yang, L.A. Herzenberg, H. Nakauchi, and L.A. Herzenberg. 2012. Distinct B-cell lineage commitment distinguishes adult bone marrow hematopoietic stem cells. *Proc. Natl. Acad. Sci. USA.* 109:5394–5398. https://doi.org/10.1073/pnas.1121632109

Ginhoux, F., and M. Guilliams. 2016. Tissue-Resident Macrophage Ontogeny and Homeostasis. *Immunity.* 44:439–449. https://doi.org/10.1016/j.immuni.2016.02.024

Han, H., K. Tanigaki, N. Yamamoto, K. Kuroda, M. Yoshimoto, T. Nakahata, K. Ikuta, and T. Honjo. 2002. Inducible gene knockout of transcription factor recombination signal binding protein-J reveals its essential role in T versus B lineage decision. *Int. Immunol.* 14:637–645. https://doi.org/10.1093/intimm/dxf030

Hara, T., S. Shitara, K. Imai, H. Miyachi, S. Kitano, H. Yao, S. Tani-ichi, and K. Ikuta. 2012. Identification of IL-7-producing cells in primary and secondary lymphoid organs using IL-7-GFP knock-in mice. *J. Immunol.* 189:1577–1584. https://doi.org/10.4049/jimmunol.1200586

Harly, C., M. Cam, J. Kaye, and A. Bhandoola. 2018. Development and differentiation of early innate lymphoid progenitors. *J. Exp. Med.* 215:249–262.

Harman, B.C., W.E. Jenkinson, S.M. Parnell, S.W. Rossi, E.J. Jenkinson, and G. Anderson. 2005. T/B lineage choice occurs prior to intrathymic Notch signaling. *Blood.* 106:886–892. https://doi.org/10.1182/blood-2004-12-4881

Hong, C., M.A. Luckey, and J.H. Park. 2012. Intrathymic IL-7: the where, when, and why of IL-7 signaling during T cell development. *Semin. Immunol.* 24:151–158. https://doi.org/10.1016/j.smim.2012.02.002

Hoyler, T., C.S. Klose, A. Souabni, A. Turqueti-Neves, D. Pfeifer, E.L. Rawlins, D. Voehringer, M. Busslinger, and A. Diefenbach. 2012. The transcription factor GATA-3 controls cell fate and maintenance of type 2 innate lymphoid cells. *Immunity.* 37:634–648. https://doi.org/10.1016/j.immuni.2012.06.020

Hozumi, K., C. Mailhos, N. Negishi, K. Hirano, T. Yahata, K. Ando, S. Zuklys, G.A. Holländer, D.T. Shima, and S. Habu. 2008. Delta-like 4 is indispensable in thymic environment specific for T cell development. *J. Exp. Med.* 205:2507–2513. https://doi.org/10.1084/jem.20080134

Huntington, N.D., H. Tabarias, K. Fairfax, J. Brady, Y. Hayakawa, M.A. Degli-Esposti, M.J. Smyth, D.M. Tarlinton, and S.L. Nutt. 2007. NK cell maturation and peripheral homeostasis is associated with KLRG1 up-regulation. *J. Immunol.* 178:4764–4770. https://doi.org/10.4049/jimmunol.178.8.4764

Ikawa, T., S. Hirose, K. Masuda, K. Kakugawa, R. Satoh, A. Shibano-Satoh, R. Kominami, Y. Katsura, and H. Kawamoto. 2010. An essential developmental checkpoint for production of the T cell lineage. *Science.* 329:93–96. https://doi.org/10.1126/science.1188995

Ishizuka, I.E., S. Chea, H. Gudjonson, and M.G. Constantinides. 2016. Single-cell analysis defines the divergence between the innate lymphoid cell lineage and lymphoid tissue-inducer cell lineage. *Nat. Immunol.* 17:269–276.

Jackson-Jones, L.H., S.M. Duncan, M.S. Magalhaes, S.M. Campbell, R.M. Maizels, H.J. McSorley, J.E. Allen, and C. Bénézech. 2016. Fat-associated lymphoid clusters control local IgM secretion during pleural infection and lung inflammation. *Nat. Commun.* 7:12651. https://doi.org/10.1038/ncomms12651

Kabata, H., K. Moro, K. Fukunaga, Y. Suzuki, J. Miyata, K. Masaki, T. Betsuyaku, S. Koyasu, and K. Asano. 2013. Thymic stromal lymphopoietin induces corticosteroid resistance in natural helper cells during airway inflammation. *Nat. Commun.* 4:2675. https://doi.org/10.1038/ncomms3675

Klose, C.S.N., M. Flach, L. Möhle, L. Rogell, T. Hoyler, K. Ebert, C. Fabiunke, D. Pfeifer, V. Sexl, D. Fonseca-Pereira, et al. 2014. Differentiation of type 1 ILCs from a common progenitor to all helper-like innate lymphoid cell lineages. *Cell.* 157:340–356. https://doi.org/10.1016/j.cell.2014.03.030

Lee, Y.H., A.P. Petkova, E.P. Mottillo, and J.G. Granneman. 2012. In vivo identification of bipotential adipocyte progenitors recruited by β3-adrenoceptor activation and high-fat feeding. *Cell Metab.* 15:480–491. https://doi.org/10.1016/j.cmet.2012.03.009

Liang, B., T. Hara, K. Wagatsuma, J. Zhang, K. Maki, H. Miyachi, S. Kitano, C. Yabe-Nishimura, S. Tani-Ichi, and K. Ikuta. 2012. Role of hepatocyte-derived IL-7 in maintenance of intrahepatic NKT cells and T cells and development of B cells in fetal liver. *J. Immunol.* 189:4444–4450. https://doi.org/10.4049/jimmunol.1201181

Lim, A.I., Y. Li, S. Lopez-Lastra, R. Stadhouders, F. Paul, A. Casrouge, N. Serafini, A. Puel, J. Bustamante, L. Surace, et al. 2017. Systemic Human ILC Precursors Provide a Substrate for Tissue ILC Differentiation. *Cell.* 168:1086–1100.e10. https://doi.org/10.1016/j.cell.2017.02.021

Ma, A., R. Koka, and P. Burkett. 2006. Diverse functions of IL-2, IL-15, and IL-7 in lymphoid homeostasis. *Annu. Rev. Immunol.* 24:657–679. https://doi.org/10.1146/annurev.immunol.24.021605.090727

Macosko, E.Z., A. Basu, R. Satija, J. Nemesh, K. Shekhar, M. Goldman, I. Tirosh, A.R. Bialas, N. Kamitaki, E.M. Martersteck, et al. 2015. Highly Parallel Genome-wide Expression Profiling of Individual Cells Using Nanoliter Droplets. *Cell.* 161:1202–1214. https://doi.org/10.1016/j.cell.2015.05.002

Mansson, R., S. Zandi, E. Welinder, P. Tsapogas, N. Sakaguchi, D. Bryder, and M. Sigvardsson. 2010. Single-cell analysis of the common lymphoid progenitor compartment reveals functional and molecular heterogeneity. *Blood.* 115:2601–2609. https://doi.org/10.1182/blood-2009-08-236398

Masuda, K., H. Kubagawa, T. Ikawa, C.C. Chen, K. Kakugawa, M. Hattori, R. Kageyama, M.D. Cooper, N. Minato, Y. Katsura, and H. Kawamoto. 2005. Prethymic T-cell development defined by the expression of paired immunoglobulin-like receptors. *EMBO J.* 24:4052–4060. https://doi.org/10.1038/sj.emboj.7600878

Miyazaki, M., H. Kawamoto, Y. Kato, M. Itoi, K. Miyazaki, K. Masuda, S. Tashiro, H. Ishihara, K. Igarashi, T. Amagai, et al. 2005. Polycomb group gene mel-18 regulates early T progenitor expansion by maintaining the expression of Hes-1, a target of the Notch pathway. *J. Immunol.* 174:2507–2516. https://doi.org/10.4049/jimmunol.174.5.2507

Miyazaki, M., K. Miyazaki, K. Chen, Y. Jin, J. Turner, A.J. Moore, R. Saito, K. Yoshida, S. Ogawa, H.R. Rodewald, et al. 2017. The E-Id Protein Axis Specifies Adaptive Lymphoid Cell Identity and Suppresses Thymic Innate Lymphoid Cell Development. *Immunity.* 46:818–834.e4. https://doi.org/10.1016/j.immuni.2017.04.022

Mjösberg, J., J. Bernink, K. Golebski, J.J. Karrich, C.P. Peters, B. Blom, A.A. te Velde, W.J. Fokkens, C.M. van Drunen, and H. Spits. 2012. The transcription factor GATA3 is essential for the function of human type 2 innate lymphoid cells. *Immunity.* 37:649–659. https://doi.org/10.1016/j.immuni.2012.08.015

Mohtashami, M., D.K. Shah, H. Nakase, K. Kianizad, H.T. Petrie, and J.C. Zúñiga-Pflücker. 2010. Direct comparison of Dll1- and Dll4-mediated Notch activation levels shows differential lymphomyeloid lineage commitment outcomes. *J. Immunol.* 185:867–876. https://doi.org/10.4049/jimmunol.1000782

Moro, K., T. Yamada, M. Tanabe, T. Takeuchi, T. Ikawa, H. Kawamoto, J. Furusawa, M. Ohtani, H. Fujii, and S. Koyasu. 2010. Innate production of T(H)2 cytokines by adipose tissue-associated c-Kit(+)Sca-1(+) lymphoid cells. *Nature.* 463:540–544. https://doi.org/10.1038/nature08636

Moro, K., K.N. Ealey, H. Kabata, and S. Koyasu. 2015. Isolation and analysis of group 2 innate lymphoid cells in mice. *Nat. Protoc.* 10:792–806. https://doi.org/10.1038/nprot.2015.047

Moro, K., H. Kabata, M. Tanabe, S. Koga, N. Takeno, M. Mochizuki, K. Fukunaga, K. Asano, T. Betsuyaku, and S. Koyasu. 2016. Interferon and IL-27 antagonize the function of group 2 innate lymphoid cells and type 2 innate immune responses. *Nat. Immunol.* 17:76–86. https://doi.org/10.1038/ni.3309

Nagasawa, T. 2007. The chemokine CXCL12 and regulation of HSC and B lymphocyte development in the bone marrow niche. *Adv. Exp. Med. Biol.* 602:69–75. https://doi.org/10.1007/978-0-387-72009-8_9

Nagasawa, T., S. Hirota, K. Tachibana, N. Takakura, S. Nishikawa, Y. Kitamura, N. Yoshida, H. Kikutani, and T. Kishimoto. 1996. Defects of B-cell lymphopoiesis and bone-marrow myelopoiesis in mice lacking the CXC chemokine PBSF/SDF-1. *Nature.* 382:635–638. https://doi.org/10.1038/382635a0

Oboki, K., T. Ohno, N. Kajiwara, K. Arae, H. Morita, A. Ishii, A. Nambu, T. Abe, H. Kiyonari, K. Matsumoto, et al. 2010. IL-33 is a crucial amplifier of innate rather than acquired immunity. *Proc. Natl. Acad. Sci. USA.* 107:18581–18586. https://doi.org/10.1073/pnas.1003059107

Possot, C., S. Schmutz, S. Chea, L. Boucontet, A. Louise, A. Cumano, and R. Golub. 2011. Notch signaling is necessary for adult, but not fetal, development of RORγt(+) innate lymphoid cells. *Nat. Immunol.* 12:949–958. https://doi.org/10.1038/ni.2105

Ramond, C., C. Berthault, O. Burlen-Defranoux, A.P. de Sousa, D. Guy-Grand, P. Vieira, P. Pereira, and A. Cumano. 2014. Two waves of distinct hematopoietic progenitor cells colonize the fetal thymus. *Nat. Immunol.* 15:27–35. https://doi.org/10.1038/ni.2782

Robbins, S.H., K.B. Nguyen, N. Takahashi, T. Mikayama, C.A. Biron, and L. Brossay. 2002. Cutting edge: inhibitory functions of the killer cell lectin-like receptor G1 molecule during the activation of mouse NK cells. *J. Immunol.* 168:2585–2589. https://doi.org/10.4049/jimmunol.168.6.2585

Rochman, Y., R. Spolski, and W.J. Leonard. 2009. New insights into the regulation of T cells by gamma(c) family cytokines. *Nat. Rev. Immunol.* 9:480–490. https://doi.org/10.1038/nri2580

Satija, R., J.A. Farrell, D. Gennert, A.F. Schier, and A. Regev. 2015. Spatial reconstruction of single-cell gene expression data. *Nat. Biotechnol.* 33:495–502. https://doi.org/10.1038/nbt.3192

Serafini, N., R.G. Klein Wolterink, N. Satoh-Takayama, W. Xu, C.A. Vosshenrich, R.W. Hendriks, and J.P. Di Santo. 2014. Gata3 drives development of RORγt+ group 3 innate lymphoid cells. *J. Exp. Med.* 211:199–208. https://doi.org/10.1084/jem.20131038

Spits, H., D. Artis, M. Colonna, A. Diefenbach, J.P. Di Santo, G. Eberl, S. Koyasu, R.M. Locksley, A.N. McKenzie, R.E. Mebius, et al. 2013. Innate lymphoid cells--a proposal for uniform nomenclature. *Nat. Rev. Immunol.* 13:145–149. https://doi.org/10.1038/nri3365

Stier, M.T., J. Zhang, K. Goleniewska, J.Y. Cephus, M. Rusznak, L. Wu, and L. Van Kaer. 2018. IL-33 promotes the egress of group 2 innate lymphoid cells from the bone marrow. *J. Exp. Med.* 215:263–281.

Tokoyoda, K., T. Egawa, T. Sugiyama, B.I. Choi, and T. Nagasawa. 2004. Cellular niches controlling B lymphocyte behavior within bone marrow during development. *Immunity.* 20:707–718. https://doi.org/10.1016/j.immuni.2004.05.001

Washburn, T., E. Schweighoffer, T. Gridley, D. Chang, B.J. Fowlkes, D. Cado, and E. Robey. 1997. Notch activity influences the alphabeta versus gammadelta T cell lineage decision. *Cell.* 88:833–843. https://doi.org/10.1016/S0092-8674(00)81929-7

Watanabe, Y., O. Mazda, Y. Aiba, K. Iwai, J. Gyotoku, S. Ideyama, J. Miyazaki, and Y. Katsura. 1992. A murine thymic stromal cell line which may support the differentiation of CD4-8- thymocytes into CD4+8- alpha beta T cell receptor positive T cells. *Cell. Immunol.* 142:385–397. https://doi.org/10.1016/0008-8749(92)90299-5

Wong, S.H., J.A. Walker, H.E. Jolin, L.F. Drynan, E. Hams, A. Camelo, J.L. Barlow, D.R. Neill, V. Panova, U. Koch, et al.. 2012. Transcription factor RORα is critical for nuocyte development. *Nat. Immunol.* 13:229–236. https://doi.org/10.1038/ni.2208 22267218

Xu, W., R.G. Domingues, D. Fonseca-Pereira, M. Ferreira, H. Ribeiro, S. Lopez-Lastra, Y. Motomura, L. Moreira-Santos, F. Bihl, V. Braud, et al. 2015. NFIL3 orchestrates the emergence of common helper innate lymphoid cell precursors. *Cell Reports.* 10:2043–2054. https://doi.org/10.1016/j.celrep.2015.02.057

Yang, Q., S.A. Saenz, D.A. Zlotoff, D. Artis, and A. Bhandoola. 2011. Cutting edge: Natural helper cells derive from lymphoid progenitors. *J. Immunol.* 187:5505–5509. https://doi.org/10.4049/jimmunol.1102039

Yang, Q., L.A. Monticelli, S.A. Saenz, A.W. Chi, G.F. Sonnenberg, J. Tang, M.E. De Obaldia, W. Bailis, J.L. Bryson, K. Toscano, et al. 2013. T cell factor 1 is required for group 2 innate lymphoid cell generation. *Immunity.* 38:694–704. https://doi.org/10.1016/j.immuni.2012.12.003

Yang, Q., F. Li, C. Harly, S. Xing, L. Ye, X. Xia, H. Wang, X. Wang, S. Yu, X. Zhou, et al. 2015. TCF-1 upregulation identifies early innate lymphoid progenitors in the bone marrow. *Nat. Immunol.* 16:1044–1050. https://doi.org/10.1038/ni.3248

Yu, X., Y. Wang, M. Deng, Y. Li, K.A. Ruhn, C.C. Zhang, and L.V. Hooper. 2014. The basic leucine zipper transcription factor NFIL3 directs the development of a common innate lymphoid cell precursor. *eLife.* 3. https://doi.org/10.7554/eLife.04406

Zook, E.C., and B.L. Kee. 2016. Development of innate lymphoid cells. *Nat. Immunol.* 17:775–782. https://doi.org/10.1038/ni.3481

Žuklys, S., A. Handel, S. Zhanybekova, F. Govani, M. Keller, S. Maio, C.E. Mayer, H.Y. Teh, K. Hafen, G. Gallone, et al. 2016. Foxn1 regulates key target genes essential for T cell development in postnatal thymic epithelial cells. *Nat. Immunol.* 17:1206–1215.